appeared to increase in hepatocyte membranes of HCV-infected livers (Fig. 4). In general, antigen retrieval is required when attempting immunohistochemical detection of claudin-1 and occludin; therefore, expression levels should be carefully evaluated. The most suitable method for antigen staining is yet to be established and a greater number of samples need to be analyzed; however, the immunohistochemistry results presented in this study may be reliable because claudin-1 staining was similar to that demonstrated by Reynolds et al. [2008]. The staining levels appeared to be able to discriminate between HCV-infected and normal livers. In this study, there was a discrepancy between mRNA and protein levels for claudin-1. While the reason for this cannot yet be definitively explained, previous studies have suggested that HCV infection could directly increase translation of claudin-1 without altering mRNA levels, and that claudin-1 expression and localization might be regulated at the level of protein phosphorylation and palmitoylation [Yamauchi et al., 2004; Van Itallie et al., 2005; Reynolds et al., 2008].

Correlation analysis of the transcriptional levels of viral entry-associated genes demonstrated significant positive correlation for LDLR versus occludin, LDLR versus claudin-1, occludin versus claudin-1, and CD81 versus SR-BI in HCV-infected and normal livers (Table III, Fig. 2). In particular, the relationship between occludin and claudin-1 (tight-junction proteins) and between CD81 and SR-BI (E2-binding receptors) could reflect their functional similarity as viral receptors. Moreover, these findings indicate that the reciprocal relationship and regulatory pathways of genes associated with viral entry in the normal liver are consistent even during HCV infection. Only the correlation between LDLR and SR-BI appeared to be induced by HCV infection (Table III, Fig. 2), although any reasons cannot be defined. Marked suppression of LDLR following HCV infection may be associated with SR-BI expression. In any case, further studies are required to elucidate the interplay between HCV and the known host factors.

Expression profiles of genes associated with HCV entry were investigated in HCV-infected and normal livers in humans. Transcription of LDLR and claudin-1 genes was significantly suppressed and that of occludin was significantly up-regulated in HCV-infected livers. The LDLR levels were inversely correlated with the serum levels of LDL-C and HCV core protein in HCV-infected livers. Correlation of elements associated with viral entry was comparable in HCV-infected and normal livers.

REFERENCES

Benedicto I, Molina-Jiménez F, Barreiro O, Maldonado-Rodríguez A, Prieto J, Moreno-Otero R, Aldabe R, López-Cabrera M, Majano PL. 2008. Hepatitis C virus envelope components alter localization of hepatocyte tight junction-associated proteins and promote occludin retention in the endoplasmic reticulum. Hepatology 48:1044–1053.

Benedicto I, Molina-Jiménez F, Bartosch B, Cosset FL, Lavillette D, Prieto J, Moreno-Otero R, Valenzuela-Fernández A, Aldabe R, López-Cabrera M, Majano PL. 2009. Tight junction-associated protein occludin is required for a postbinding step in hepatitis C virus entry and infection. J Virol 83:8012–8020.

Brazzoli M, Bianchi A, Filippini S, Weiner A, Zhu Q, Pizza M, Crotta S. 2008. CD81 is a central regulator of cellular events required for hepatitis C virus infection of human hepatocytes. J Virol 82:8316–8329.

Brown MS, Goldstein JL. 1981. Lowering plasma cholesterol by raising LDL receptors. N Engl J Med 305:515–517.

Burlone ME, Budkowska A. 2009. Hepatitis C virus cell entry: Role of lipoproteins and cellular receptors. J General Virol 90:1055–1070.

Chen L, Borozan I, Milkiewicz P, Sun J, Meng X, Coltescu C, Edwards AM, Ostrowski MA, Guindi M, Heathcote EJ, McGilvray ID. 2008. Gene expression profiling of early primary biliary cirrhosis: Possible insights into the mechanism of action of ursodeoxycholic acid. Liver Int 28:997–1010.

Cukierman L, Meertens L, Bertaux C, Kajumo F, Dragic T. 2009. Residues in a highly conserved claudin-1 motif are required for hepatitis C virus entry and mediate the formation of cell–cell contacts. J Virol 83:5477–5484.

Durand T, Di Liberto G, Colman H, Cammas A, Boni S, Marcellin P, Cahour A, Vagner S, Feray C. 2010. Occult infection of peripheral B cells by hepatitis C variants which have low translational efficiency in cultured hepatocytes. Gut 59:934–942.

Economou M, Milionis H, Filis S, Baltayiannis G, Christou L, Elisaf M, Tsianos E. 2008. Baseline cholesterol is associated with the response to antiviral therapy in chronic hepatitis C. J Gastroenterol Hepatol 23:586–591.

Evans MJ, von Hahn T, Tscherne DM, Syder AJ, Panis M, Wölk B, Hatziioannou T, McKeating JA, Bieniasz PD, Rice CM. 2007. Claudin-1 is a hepatitis C virus co-receptor required for a late step in entry. Nature 446:801–805.

Goldstein JL, Brown MS. 1990. Regulation of the mevalonate pathway. Nature 343:425–430.

Goldstein JL, Brown MS. 2009. The LDL receptor. Arterioscler Thromb Vasc Biol 29:431–438.

Harris HJ, Farquhar MJ, Mee CJ, Davis C, Reynolds GM, Jennings A, Hu K, Yuan F, Deng H, Hubscher SG, Han JH, Balfe P, McKeating JA. 2008. CD81 and claudin 1 coreceptor association: Role in hepatitis C virus entry. J Virol 82:5007–5020.

Harris HJ, Davis C, Mullins JG, Hu K, Goodall M, Farquhar MJ, Mee CJ, McCaffrey K, Young S, Drummer H, Balfe P, McKeating JA. 2010. Claudin association with CD81 defines hepatitis C virus entry. J Biol Chem 285:21092–21102.

Huang H, Sun F, Owen DM, Li W, Chen Y, Gale M Jr, Ye J. 2007. Hepatitis C virus production by human hepatocytes dependent on assembly and secretion of very low density lipoproteins. Proc Natl Acad Sci USA 104:5848–5853.

Krieger SE, Zeisel MB, Davis C, Thumann C, Harris HJ, Schnober EK, Mee C, Soulier E, Royer C, Lambotin M, Grunert F, Dao Thi VL, Dreux M, Cosset FL, McKeating JA, Schuster C, Baumert TF. 2010. Inhibition of hepatitis C virus infection by anti-claudin-1 antibodies is mediated by neutralization of E2-CD81-claudin-1 associations. Hepatology 51:1144–1157.

Levy S, Shoham T. 2005. The tetraspanin web modulates immune-signaling complexes. Nat Rev Immunol 5:136–148.

Liu S, Yang W, Shen L, Turner JR, Coyne CB, Wang T. 2009. Tight junction proteins claudin-1 and occludin control hepatitis C virus entry and are downregulated during infection to prevent superinfection. J Virol 83:2011–2014.

Nakagawa A, Nagaoka K, Hirose T, Tsuda K, Hasegawa K, Shiratsuchi A, Nakanishi Y. 2004. Expression and function of class B scavenger receptor type I on both apical and basolateral sides of the plasma membrane of polarized testicular Sertoli cells of the rat. Dev Growth Differ 46:283–298.

Nakamuta M, Yada R, Fujino T, Yada M, Higuchi N, Tanaka M, Miyazaki M, Kohjima M, Kato M, Yoshimoto T, Harada N, Taketomi A, Maehara Y, Koga M, Nishinakagawa T, Nakashima M, Kotoh K, Enjoji M. 2009. Changes in the expression of cholesterol metabolism-associated genes in HCV-infected liver: A novel target for therapy? Int J Mol Med 24:825–828.

Owen DM, Huang H, Ye J, Gale M Jr. 2009. Apolipoprotein E on hepatitis C virion facilitates infection through interaction with low-density lipoprotein receptor. Virology 394:99–108.

Perlemuter G, Sabile A, Letteron P, Vona G, Topilco A, Chrétien Y, Koike K, Pessayre D, Chapman J, Barba G, Bréchot C. 2002.

Hepatitis C virus core protein inhibits microsomal triglyceride transfer protein activity and very low density lipoprotein secretion: A model of viral-related steatosis. FASEB J 16:185–194.

Perrault M, Pécheur EI. 2009. The hepatitis C virus and its hepatic environment: A toxic but finely tuned partnership. Biochem J 423: 303–314.

Pietschmann T. 2009. Final entry key for hepatitis C. Nature 457:797–798.

Ploss A, Evans MJ, Gaysinskaya VA, Panis M, You H, de Jong YP, Rice CM. 2009. Human occludin is a hepatitis C virus entry factor required for infection of mouse cells. Nature 457:882–886.

Reynolds GM, Harris HJ, Jennings A, Hu K, Grove J, Lalor PF, Adams DH, Balfe P, Hübscher SG, McKeating JA. 2008. Hepatitis C virus receptor expression in normal and diseased liver tissue. Hepatology 47:418–427.

Sezaki H, Suzuki F, Akuta N, Yatsuji H, Hosaka T, Kobayashi M, Suzuki Y, Arase Y, Ikeda K, Miyakawa Y, Kumada H. 2009. An open pilot study exploring the efficacy of fluvastatin, pegylated interferon and ribavirin in patients with hepatitis C virus genotype 1b in high viral load. Intervirology 52:43–48.

Stamataki Z. 2010. Hepatitis C infection of B lymphocytes: More tools to address pending questions. Expert Rev Anti Infect Ther 8:977–980.

Syed GH, Amako Y, Siddiqui A. 2010. Hepatitis C virus hijacks host lipid metabolism. Trends Endocrinol Metab 21:33–40.

Tang H, Grisé H. 2009. Cellular and molecular biology of HCV infection and hepatitis. Clin Sci 117:49–65.

Torres DM, Harrison SA. 2008. HCV replication and statin pleotropism: An adjuvant treatment panacea? Am J Gastroenterol 103: 1390–1392.

Van Itallie CM, Gambling TM, Carson JL, Anderson JM. 2005. Palmitoylation of claudins is required for efficient tight-junction localization. J Cell Sci 118:1427–1436.

Yamauchi K, Rai T, Kobayashi K, Sohara E, Suzuki T, Itoh T, Suda S, Hayama A, Sasaki S, Uchida S. 2004. Disease-causing mutant WNK4 increases paracellular chloride permeability and phosphorylates claudins. Proc Natl Acad Sci USA 101:4690–4694.

Yang W, Qiu C, Biswas N, Jin J, Watkins SC, Montelaro RC, Coyne CB, Wang T. 2008. Correlation of the tight junction-like distribution of claudin-1 to the cellular tropism of hepatitis C virus. J Biol Chem 283:8643–8653.

J Gastroenterol (2011) 46:705–711
DOI 10.1007/s00535-010-0365-7

ORIGINAL ARTICLE—LIVER, PANCREAS, AND BILIARY TRACT

New method for assessing liver fibrosis based on acoustic radiation force impulse: a special reference to the difference between right and left liver

Takeo Toshima · Ken Shirabe · Kazuki Takeishi · Takashi Motomura · Youhei Mano · Hideaki Uchiyama · Tomoharu Yoshizumi · Yuji Soejima · Akinobu Taketomi · Yoshihiko Maehara

Received: 27 July 2010 / Accepted: 13 December 2010 / Published online: 26 January 2011

Abstract
Background Virtual touch tissue quantification (VTTQ) based on acoustic radiation force impulse (ARFI) imaging has been developed as a noninvasive bedside method for the assessment of liver stiffness. In this study, we examined the diagnostic performance of ARFI imaging in 103 patients, focusing on the difference in VTTQ values between the right and left liver lobes.
Methods We evaluated VTTQ values of the right and left lobes in 79 patients with chronic liver disease who underwent histological examination of liver fibrosis and in 24 healthy volunteers. The diagnostic accuracy of VTTQ was compared with several serum markers, including hyaluronic acid, type 4 collagen, and aspartate transaminase to platelet ratio index.
Results The VTTQ values (meters per second) in the right and left lobes were 1.61 ± 0.51 and 1.90 ± 0.68, respectively, and the difference was statistically significant ($P < 0.0001$). The VTTQ values in both liver lobes were correlated significantly with histological fibrosis grades ($P < 0.001$). The standard deviations of the VTTQ values in the right lobe were significantly lower than those in the left lobe ($P < 0.001$). The area under the receiver-operating characteristic curve for the diagnosis of fibrosis ($F \geq 3$) using VTTQ values in both liver lobes was superior to serum markers, especially in the right lobe.
Conclusions VTTQ is an accurate and reliable tool for the assessment of liver fibrosis. VTTQ of the right lobe was more accurate for diagnosing liver fibrosis than in the left lobe.

Keywords Virtual touch tissue quantification · Acoustic radiation force impulse · Liver fibrosis · Transient elastography · Chronic hepatitis

Abbreviations

VTTQ	Virtual Touch^{TM} tissue quantification
ARFI	Acoustic radiation force impulse
ROC	Receiver operating characteristic
ALT	Alanine aminotransferase
LDLT	Living donor liver transplantation
APRI	Aspartate transaminase-to-platelet ratio index
HCVAb	Hepatitis C virus antibody
HBsAg	Hepatitis B virus surface antigen
m/s	Meters per second
AST	Aspartate aminotransferase
PPV	Positive predictive value
NPV	Negative predictive value
HBV	Hepatitis B virus
HCV	Hepatitis C virus

Introduction

The management of chronic liver disease depends on the degree of liver fibrosis, and therefore, the assessment of the degree of liver fibrosis is important for choosing a therapeutic strategy and for determining the prognosis [1, 2]. Liver biopsy has been the gold standard method for

T. Toshima (✉) · K. Shirabe · K. Takeishi · T. Motomura · Y. Mano · H. Uchiyama · T. Yoshizumi · Y. Soejima · A. Taketomi · Y. Maehara
Department of Surgery and Science, Graduate School of Medical Sciences, Kyushu University, 3-1-1 Maidashi, Higashi-ku, Fukuoka 812-8582, Japan
e-mail: toshima@surg2.med.kyushu-u.ac.jp

evaluating the degree of liver fibrosis [3]. However, its invasiveness, potential for life-threatening complications, and sampling errors place a heavy burden on those patients with hepatitis who require follow-up [4–6]. Therefore, noninvasive examination methods for assessing the degree of liver fibrosis, such as serum markers and transient elastography (FibroScan®, Echosens, Paris, France), have been proposed and tried [7–9].

Recently, a method based on acoustic radiation force impulse (ARFI) imaging, Virtual Touch™ tissue quantification (VTTQ), has been introduced to evaluate organ stiffness. The mechanism of VTTQ measurement exploits the phenomena whereby lower displacement magnitudes are induced in cirrhotic liver tissue compared with those induced in noncirrhotic liver tissue, as reported by Nightingale et al. [10]. VTTQ measurements can be performed during observation of a particular liver lesion with an ultrasonic probe, and measurements may be reproducible when compared with transient elastography.

In two pilot studies, it was concluded that liver VTTQ based on ARFI might be useful for the assessment of liver fibrosis in patients with chronic liver disease [11, 12]. In each study, the areas under the receiver-operating characteristic (ROC) curves for F2 were 0.82 and 0.94. However, the number of patients studied was <100, and both study groups were comprised of hepatitis patients, including hepatitis C virus (HCV). Regardless, we observed significant differences in VTTQ values between the right and left lobes of the liver, although this finding has not been reported.

To our knowledge, this is the first report to quantify liver fibrosis stiffness in both the right and left lobe of the liver by VTTQ examination in a study size >100. In this study, we compared the diagnostic accuracy of VTTQ in both the right and left lobes of the liver, using the area under the ROC curves. Furthermore, the diagnostic performance of VTTQ was compared with validated serum fibrosis markers, including the levels of hyaluronic acid and type 4 collagen, and the aspartate transaminase-to-platelet ratio index (APRI).

Patients and methods

Patients

We consecutively enrolled 103 adults, including 24 healthy volunteers (control; $n = 24$) and 79 patients with or without hepatitis who underwent hepatectomy or living donor liver transplantation (LDLT) and who were measured by VTTQ in the right and the left liver at Kyushu University Hospital. Of these, 73 patients underwent hepatic resection for hepatocellular carcinoma; 46 of these expressed the hepatitis C virus antibody (HCVAb), 7 were positive for hepatitis B virus surface antigen (HBsAg), and 3 were due to alcohol. One patient underwent hepatic resection as a donor for LDLT, and five patients underwent hepatic resection as a recipient. The study protocol conformed to the ethics guidelines of the 1975 Helsinki Declaration and was approved by our institutional review board.

Liver histology and quantification of liver fibrosis

All liver specimens were obtained by surgical resection and were fixed in formalin, embedded in paraffin wax, and stained with hematoxylin and eosin and Masson's trichrome. The fibrosis staging in all surgical specimens was determined independently by two pathologists who did not know the VTTQ values. In case of discrepancies, histological sections were simultaneously reviewed using a multi-pipe microscope to reach a consensus. Fibrosis staging was scored using the Scheuer classification [16] on a scale of 0–4 as follows: F0, no fibrosis; F1, enlarged, fibrotic portal tracts; F2, periportal or portal-portal septa but intact architecture; F3, fibrosis with architectural distortion but no obvious cirrhosis; F4, probable or definite cirrhosis.

Virtual touch tissue quantification and acoustic radiation force impulse

The VTTQ system was installed on an ACUSON model S2000 ultrasound system (Siemens Medical Solutions Inc., Ultrasound Division, Issaquah, WA). The operators were surgeons trained by Siemens Medical Solutions Inc. The VTTQ system utilizes an acoustic push pulse to generate shear waves, which pass through the liver parenchyma orthogonally to the acoustic push pulse, through a user-placed region of interest. When detection pulses interact with a passing shear wave, they reveal the wave's location at a specific time, allowing calculation of the shear wave speed. This absolute numerical value is related to the stiffness of the tissue within the region of interest [13–15], and the results are expressed in meters per second (m/s). For each patient, seven successful measurements were performed several days before surgical operations, during which the histological specimens were obtained. A total of 1442 measurements were performed in a total of 103 patients, including 721 measurements in both lobes, respectively. The measurement of VTTQ in the right lobe of the liver was performed by placing the ultrasonic probe on the right intercostal space, and in the left lobe of the liver, measurement was performed by placing the probe under the xiphoid process of the sternum at a depth from 2 to 4 cm. The median value of all measurements and the

standard deviation of all right and left VTTQ measurements for each patient were considered for analysis.

Surrogate serum markers

For all patients, blood samples were obtained on the same day that the VTTQ examination was performed and were examined in the same laboratory. The following parameters were determined: levels of hyaluronic acid, type 4 collagen, platelet count, aspartate aminotransferase (AST), alanine aminotransferase (ALT), and APRI. The APRI was calculated as follows: AST level (per upper limit of normal; 33 U/l) × 100/platelet count (10^9/l) [16, 17].

Statistical analysis

Differences between quantitative variables for paired samples were analyzed using a nonparametric test (Wilcoxon rank sum test with Bonferroni's adjustment). The sensitivity, specificity, positive predictive value (PPV), and negative predictive value (NPV) of liver stiffness optimal cutoff values for the diagnosis of liver fibrosis were calculated, as previously published [16, 17]. In addition, the diagnostic value of liver stiffness for predicting significant liver fibrosis (F1–F3) and cirrhosis (F4) was assessed by calculating the areas under the ROC curves. The ROC curve is a plot of sensitivity versus 1-specificity for all possible cutoff values. The most commonly used index of accuracy is the area under the ROC curve, where values close to 1.0 indicate high diagnostic accuracy, and 0.5 indicates a test of no diagnostic value. The optimal liver stiffness cutoff values used for the diagnosis of significant fibrosis and cirrhosis were selected based on the sensitivity, specificity, PPV, and NPV [16, 17, 19]. Statistical analysis of the differences between the areas under the ROC curves was based on the theory of generalized *U*-statistics [20]. All of the differences were considered statistically significant at $P < 0.05$.

Results

Patients and liver specimens

Patient characteristics are summarized in Table 1. The mean age of the patients (69 men and 34 women) was 66 ± 12 years. The number of healthy volunteers for the control was 24 and the etiology of hepatitis for 79 patients was classified as follows: hepatitis C (HCV; $n = 46$), hepatitis B (HBV; $n = 7$), alcohol ($n = 3$), and etiology unknown ($n = 23$). In the patients whose etiology of hepatitis was unknown, HCVAb, HBsAg, and hepatitis B core antibody were negative, and alcoholic hepatitis and nonalcoholic steatohepatitis were not diagnosed clinically.

Table 1 Patient characteristics

Characteristics	Mean ± SE
Sex (men/women)	69/34
Age (years)	66 ± 12
Etiology of hepatitis; control/HCVAb (+)/HBsAg (+)/alcohol/unknown	24/46/7/3/23
AST level (U/l)	48.0 ± 37.1
ALT level (U/l)	39.8 ± 31.5
Platelet ($\times 10^4$/μl)	16.2 ± 7.8
Hyaluronic acid (ng/ml)	176.8 ± 148.0
Type 4 collagen (ng/ml)	214.4 ± 84.1
APRI	0.43 ± 0.51
Fibrosis grade F; control/0/1/2/3/4	24/12/15/16/15/21

HBsAg hepatitis B surface antigen, *HCVAb* hepatitis C viral antibody, *AST* aspartate transaminase, *ALT* alanine aminotransferase, *APRI* aspartate transaminase-to-platelet ratio index

The fibrosis grades of the 79 surgical liver specimens were as follows: F0, $n = 12$; F1, $n = 15$; F2, $n = 16$; F3, $n = 15$; F4, $n = 21$, and control, $n = 24$.

Liver stiffness by virtual touch tissue quantification

Figure 1 shows box plots of the VTTQ values for each fibrosis stage, for VTTQ values of the right lobe of the liver (Fig. 1a) and left lobe of the liver (Fig. 1b). Liver stiffness values measured by shear wave velocity ranged from 0.74 to 2.88 m/s for the right lobe of the liver and from 0.84 to 3.83 m/s for the left lobe of the liver. The VTTQ values (right/left) in patients with fibrosis grade control ($n = 24$), F0 ($n = 12$), F1 ($n = 15$), F2 ($n = 16$), F3 ($n = 15$), and F4 ($n = 21$) were 1.15/1.41, 1.18/1.41, 1.51/1.85, 1.57/1.77, 1.85/1.88, and 2.10/2.66 m/s, respectively. There were significant correlations between the fibrosis stage and both right and left liver stiffness values ($P < 0.001$). The VTTQ value (1.61 ± 0.51) of the right lobe of the liver was lower than that of the left lobe of the liver (1.90 ± 0.68), and the difference was statistically significant ($P < 0.0001$) (Table 2). The standard deviation of VTTQ values in the right lobe (0.23 ± 0.18) was significantly lower than that of the left lobe (0.30 ± 0.17) ($P < 0.001$). The cutoff values were determined as described above [16, 17]. The optimal cutoff values (right/left) were 1.45/1.84 m/s for $F \geq 1$, 1.52/2.16 m/s for $F \geq 2$, 1.69/2.24 m/s for $F \geq 3$, and 1.79/2.38 m/s for $F \geq 4$ (Tables 3, 4). The areas under the ROC curve for the diagnosis of fibrosis types F1, F2, F3, and F4 with the right lobe VTTQ value were 0.81, 0.81, 0.85, and 0.87, respectively (Fig. 2a), and with the left lobe VTTQ value were 0.69, 0.71, 0.76, and 0.86, respectively (Fig. 2b). The area under the ROC curve for the diagnosis of fibrosis ($F \geq 1$) with the right lobe VTTQ value was significantly

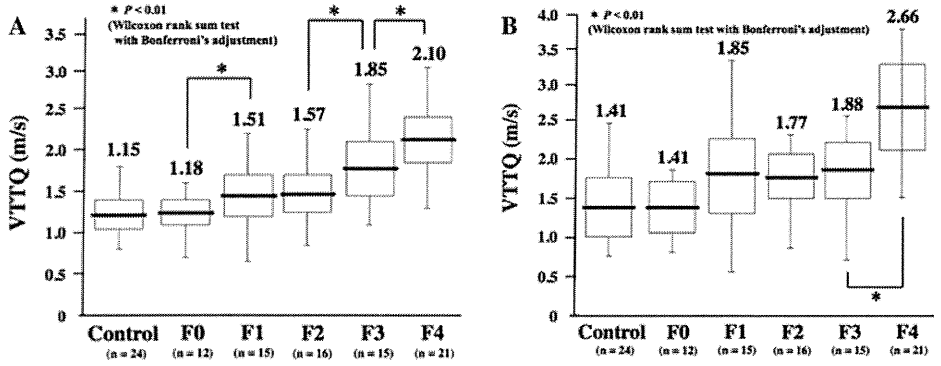

Fig. 1 Box-and-whisker plot of the VTTQ values for each fibrosis stage. Liver stiffness values measured by shear wave velocity for the right liver lobe (**a**) and for the left liver lobe (**b**). The *tops* and *bottoms* of the *boxes* represent the first and third quartiles, respectively. The *length of the box* thus represents the interquartile range, covering 50% of the values. The *line through the middle of each box* represents the median. The *error bars* show the minimum and maximum values (range). Significant correlations were found between the stage of fibrosis and liver stiffness. Statistically significant by the Wilcoxon rank sum test with Bonferroni's adjustment; $*P < 0.01$

Table 2 The difference between right and left lobe VTTQ values

$n = 103$	Right lobe VTTQ	Left lobe VTTQ	P value
VTTQ value for each patient	1.61 ± 0.51	1.90 ± 0.68	<0.0001
Standard deviation of all VTTQ values for each patient	0.23 ± 0.18	0.30 ± 0.17	<0.001

The VTTQ values of those 103 patients who were assessed in both the right and left lobes of the liver

Table 3 Liver stiffness values (right lobe)

Values (right lobe)	$F \geq 1$	$F \geq 2$	$F \geq 3$	$F \geq 4$
Optimal cutoff (m/s)	1.45	1.52	1.69	1.79
Sensitivity	0.70	0.75	0.78	0.86
Specificity	0.78	0.76	0.84	0.79
PPV	0.85	0.76	0.72	0.51
NPV	0.58	0.75	0.88	0.95

Optimal cutoff points gave the highest total sensitivity and specificity

m/s meters per second, *PPV* positive predictive value, *NPV* negative predictive value

Table 4 Liver stiffness values (left lobe)

Values (left lobe)	$F \geq 1$	$F \geq 2$	$F \geq 3$	$F \geq 4$
Optimal cutoff (m/s)	1.84	2.16	2.24	2.38
Sensitivity	0.62	0.52	0.58	0.67
Specificity	0.78	0.84	0.84	0.89
PPV	0.85	0.77	0.62	0.61
NPV	0.56	0.63	0.83	0.91

Optimal cutoff points gave the highest total sensitivity and specificity

m/s meters per second, *PPV* positive predictive value, *NPV* negative predictive value

higher than for the left lobe VTTQ value ($P < 0.05$), and the statistical significance was investigated for the diagnosis of fibrosis ($F \geq 2$ and $F \geq 3$) ($P < 0.05$). The area under the ROC curve for each point with the right lobe VTTQ was higher than with the left lobe VTTQ.

Comparison of virtual touch tissue quantification with serum markers for the diagnosis of fibrosis stage ≥3

We compared the area under the ROC curve of the serum markers (hyaluronic acid, type 4 collagen, and APRI) with that of the right lobe VTTQ values, as it was superior to the left VTTQ values for the diagnosis of all fibrosis types. The cutoff values were determined as described before. The optimal cutoff values were 1.69 m/s for the right VTTQ, 2.24 m/s for the left VTTQ, 218.0 ng/ml for hyaluronic acid, 214.0 ng/ml for type 4 collagen, and 0.24 for APRI for the diagnosis of fibrosis stage ≥3 (Table 5). The areas under the ROC curves for the diagnosis of fibrosis ($F \geq 3$) according to the right lobe VTTQ, the left lobe VTTQ, hyaluronic acid, type 4 collagen, and APRI cutoff measures were 0.85, 0.76, 0.77, 0.65, and 0.75, respectively (Fig. 3).

Discussion

This is the first report to quantify liver fibrosis in both the right and left lobes of the liver in a large population

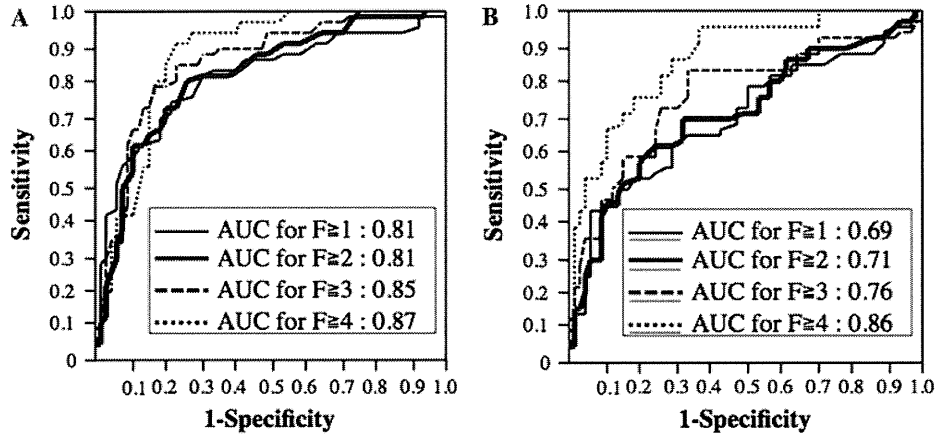

Fig. 2 Diagnostic value of the right VTTQ and the left VTTQ to assess the stage of the liver fibrosis. **a** The receiver-operating (ROC) curves by the right VTTQ for diagnosing liver fibrosis grade $F \geq 1$ (*thin black line*, area under curve = 0.81), $F \geq 2$ (*bold black line*, area under curve = 0.81), $F \geq 3$ (*dashed line*, area under curve = 0.85) and $F \geq 4$ (*dotted line*, area under curve = 0.87) are shown. **b** The receiver operating (ROC) curves by the left VTTQ for diagnosing liver fibrosis grade $F \geq 1$ (*thin black line*, area under curve = 0.69), $F \geq 2$ (*bold black line*, area under curve = 0.71), $F \geq 3$ (*dashed line*, area under curve = 0.76) and $F \geq 4$ (*dotted line*, area under curve = 0.86) are shown

Table 5 Diagnostic performance for predicting liver fibrosis ($F \geq 3$)

	VTTQ (right lobe)	VTTQ (left lobe)	Hyaluronic acid	Type 4 collagen	APRI
Optimal cutoff (unit)	1.69 (m/s)	2.24 (m/s)	218 (ng/mL)	214 (ng/mL)	0.24
Sensitivity	0.78	0.58	0.67	0.60	0.69
Specificity	0.84	0.84	0.94	0.71	0.72
PPV	0.72	0.62	0.89	0.60	0.57
NPV	0.88	0.83	0.78	0.71	0.81

VTTQ Virtual Touch^{TM} tissue quantification, *APRI* aspartate transaminase-to-platelet ratio index, *PPV* positive predictive value, *NPV* negative predictive value

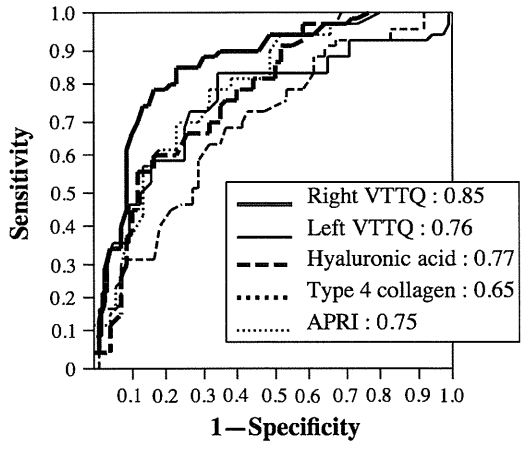

Fig. 3 Areas under the ROC curves for diagnosing fibrosis grade $F \geq 3$ by the VTTQ in the right lobe of the liver, the VTTQ in the left lobe of the liver, and serum levels of hyaluronic acid, type 4 collagen, and APRI. Shown are the ROC curves for diagnosis using the right VTTQ (*bold black line*, area under curve = 0.85), the left VTTQ (*thin black line*, area under curve = 0.76), hyaluronic acid level (*bold dashed line*, area under the curve = 0.77), type 4 collagen level (*bold dotted line*, area under the curve = 0.65), and APRI (*thin dotted line*, area under the curve = 0.75)

($n = 103$) using the VTTQ examination method. The accuracy of right and left lobe VTTQ values for diagnosing liver fibrosis grade $F \geq 3$, measured as sensitivity, specificity, PPV, and NPV, was better than serum markers of liver fibrosis, such as the levels of hyaluronic acid, type 4 collagen, and the APRI. This finding is supported by previously reported preliminary data [11, 12].

Many studies have demonstrated that measurement of liver stiffness by transient elastography using FibroScan is a valuable method for assessing liver fibrosis [16–18], and we have previously demonstrated the feasibility of FibroScan for patients with recurrent HCV after LDLT [17]. However, this approach has some limitations when compared with the VTTQ method. First, transient elastography using FibroScan is performed in a blind fashion [17]. Indeed, FibroScan includes a TM screen that shows the ultrasonographic view of the region of interest. However, only large vessels can be distinguished in the image displayed with TM mode in comparison with the B mode standard ultrasonographic image obtained by VTTQ. In most of the previous studies that employed FibroScan, the authors have stated that regions with large vessels were

avoided, and a minimal liver parenchyma thickness of 6 cm was sought to minimize the error [16–18]. Nevertheless, these types of acquisition errors can occur because this approach is performed in a blind fashion. This could be the major advantage of VTTQ over transient elastography using FibroScan for the assessment of liver fibrosis. Second, previous reports of elastography in large numbers of the patients have demonstrated that cutoff values between F2 and F3 were close [16–19]. The low predictive value of F2 and F3 could be another limitation of the FibroScan-based elastography. Patients with liver fibrosis of grade F3 or cirrhosis have greater risk of developing hepatocellular carcinoma than those with a liver fibrosis of grade F2. In a study of 2890 patients with hepatitis, Yoshida et al. [21] reported that the annual carcinogenesis rate was correlated with the stage of liver fibrosis. Whereas the annual incidence of hepatocellular carcinoma in patients with severe liver fibrosis of grade F3 was high at 5.3%, the incidence in those with moderate liver fibrosis of grade F2 was low at 1.9%. Furthermore, those patients with a liver fibrosis of grade F3 tended to progress to cirrhosis more easily than those with grade F2 disease. According to a study of 1500 patients with HCV-related chronic hepatitis, Ikeda et al. [22] reported that the progression rate to cirrhosis in patients with liver fibrosis grade F2 was 6.1%, whereas those with liver fibrosis grade F3 was very high at 50.2%, as measured at the end of the 10th year from the start of the observation. They concluded that the fibrotic change was closely correlated with the disease progression rate in patients with viral hepatitis. These findings all suggest that it is critically important to distinguish between liver fibrosis of grade F3 and F2.

Previous studies have not paid much attention to the probe position and the points of measurement when assessing liver fibrosis by VTTQ, as operators are free to measure organ stiffness at any point if they want. Nevertheless, the results of this study suggest that VTTQ measurement with the right lobe is more accurate than with the left lobe when assessing liver fibrosis. The actual values of VTTQ for the right lobe were significantly lower than for the left lobe. The standard deviation of the measured values with the right lobe was significantly lower than with the left lobe. Furthermore, the area under the ROC curve for diagnosing liver fibrosis by the right lobe VTTQ measurement was significantly higher than with the left lobe VTTQ.

Next, we examined the relationship between liver fibrosis stage and VTTQ value in the same lobe of the liver. The lobes of the 79 surgical liver specimens were as follows: right, $n = 44$ and left, $n = 37$. The areas under the ROC curve for the diagnosis of fibrosis types F1, F2, F3, and F4 in the right lobe by right VTTQ value ($n = 44$) were 0.92, 0.83, 0.86, and 0.80, and in the left lobe by left VTTQ value ($n = 37$) were 0.77, 0.71, 0.78, and 0.84, respectively. The ability to diagnose fibrosis of stage ≥ 3, which involves sensitivity, specificity, PPV, and NPV, in the right lobe by right VTTQ value were 0.88, 0.81, 0.74, and 0.92, and in the left lobe by left VTTQ value were 0.80, 0.75, 0.87, and 0.68, respectively. Considering these results, it may be concluded that the right VTTQ examination was more accurate for the diagnosis of liver fibrosis than the left VTTQ examination. The cause for this difference remains unknown. The higher standard deviation of the left lobe VTTQ values compared with the right lobe VTTQ values suggests that there may be some difficulties with measurement of VTTQ in the left lobe.

The anatomical features of the left lobe of the liver may have an influence on the measurement of VTTQ. The left lobe is surrounded by the diaphragm, stomach, and aorta, and so may be influenced by respiratory fluctuations, the presence of food in the stomach, and the pulsation of the aorta, respectively. Another factor may be the probe's position. Few studies of the measurement of liver stiffness using Fibroscan have examined the variability that is possible with different positions of the probe [23]. In almost all of the studies employing FibroScan, the described method was taken from the original description by Sandrin et al. [24], "because liver biopsies are performed on the right lobe of the liver, so were the elasticity measurements. During the acquisition, patients were lying on their backs with their right arms behind their heads. The physician first proceeded to a sonographic examination to localize the best ultrasonic imaging window between the rib bones." Recently, Ingiliz et al. [23] demonstrated two major points to consider regarding the significance of the probe position and the influence of the skin fold thickness when assessing liver stiffness. First, they showed that the anterior position of the probe should be the first choice for liver stiffness measurement using Fibroscan, as it has a higher applicability without higher variability as compared with the usual liver biopsy position. By contrast, in VTTQ measurements, organ stiffness can be measured at any point that the operators desire because the ultrasonography can be performed during acquisition, and vessels and liver parenchyma thickness are not related to the VTTQ values. Second, in their multivariate analysis, only thoracic skin fold was significantly associated with the variability of the right liver stiffness. Considering this result, the difference in the skin thicknesses between the skin on the right intercostal space and under the xiphoid process of the sternum may be due to the difference in VTTQ between the right and left lobe, and further examination is necessary.

In conclusion, VTTQ examination based on ARFI imaging is an accurate, reliable, reproducible, and noninvasive method with which to assess liver fibrosis of both the right and left lobe of the liver. This approach can be

performed with simultaneous observation of individual liver lesions using ultrasonography. The VTTQ measurement of the right lobe may be superior to that of the left lobe for the diagnosis of liver fibrosis, and it may be valuable when assessing patients in whom taking a liver biopsy would be risky, such as those with liver cirrhosis.

Acknowledgments The authors wish to thank Siemens Medical Solutions USA, Inc., for the use of the Acuson S2000 device, Mochida Siemens Medical Systems Co., Ltd., in Japan for assisting in the setup of the device, and Ms. Natsumi Yamashita for her valuable advice with the statistical analysis. We have no financial interests linked to this work.

References

1. Mazzagferro V, Regalia E, Doci R, Andreola S, Pulvirenti A, Bozzetti F, et al. Liver transplantation for the treatment of small hepatocellular carcinomas in patients with cirrhosis. N Engl J Med. 1996;334:693–9.
2. National Institutes of Health. NIH consensus statement on management of hepatitis C. Hepatology. 2002;36:S3–20.
3. Bravo AA, Sheth SG, Chopra S. Liver biopsy. N Engl J Med. 2001;344:495–500.
4. Maharaj B, Maharaj RJ, Leary WP, Cooppan RM, Naran AD, Pirie D, et al. Sampling variability and its influence on the diagnostic yield of percutaneous needle biopsy of the liver. Lancet. 1986;1:523–5.
5. Regev A, Berho M, Jeffers LJ, Milikowski C, Molina EG, Pyrsopoulos NT, et al. Sampling error and intraobserver variation in liver biopsy in patients with chronic HCV infection. Am J Gastroenterol. 2002;97:2614–8.
6. Bedossa P, Dargere D, Paradise V. Sampling variability of liver fibrosis in chronic hepatitis C. Hepatology. 2003;38:1449–57.
7. Imbert-Bismut F, Ratziu V, Pieroni L, Charlotte F, Benhamou Y, Poynard T, et al. Biochemical markers of liver fibrosis in patients with hepatitis C virus infection: a prospective study. Lancet. 2001;357:1069–75.
8. Forns X, Ampurdanes S, Llovet JM, Aponte J, Quinto L, Martinez-Bauer E, et al. Identification of chronic hepatitis C patients without hepatic fibrosis by a simple predictive model. Hepatology. 2002;36:986–92.
9. Guechot J, Laudat A, Loria A, Serfaty L, Poupon R, Giboudeau J. Diagnostic accuracy of hyaluronans and type III procollagen aminoterminal peptide serum assays as markers of liver fibrosis in chronic viral hepatitis C evaluated by ROC curve analysis. Clin Chem. 1996;42:558–63.
10. Nightingale KR, Zhai L, Dahl JJ, Frinkley KD, Palmeri ML. Shear wave velocity estimation using acoustic radiation force impulsive excitation in liver in vivo. In: Proceedings of institute of electrical and electronics engineers (IEEE) ultrasonics symposium, 2006. Vancouver: IEEE; 2006. p. 1156–60.
11. Friedrich-Rust M, Wunder K, Kriener S, Sotoudeh F, Richter S, Bojunga J, et al. Liver fibrosis in viral hepatitis: noninvasive assessment with acoustic radiation force impulse imaging versus transient elastography. Radiology. 2009;252:595–604.
12. Takahashi H, Ono N, Eguchi Y, Eguchi T, Kitajima Y, Kawaguchi Y, et al. Evaluation of acoustic radiation force impulse elastography for fibrosis staging of chronic liver disease: a pilot study. Liver Int. 2010;30:538–45.
13. Palmeri ML, Frinkley KD, Zhai L, Gottfried M, Bentley RC, Ludwig K, et al. Acoustic radiation force impulse (ARFI) imaging of the gastrointestinal tract. IEEE. 2004;1:23–7.
14. Dahl JJ, Pinton GF, Palmeri ML, Agrawal V, Nightingale KR, Trahey GE. A parallel tracking method for acoustic radiation force impulse imaging. IEEE Trans Ultrason Ferroelectr Freq Control. 2007;54:301–12.
15. Garra BS. Imaging and estimation of tissue elasticity by ultrasound. Ultrasound Q. 2007;23:255–68.
16. Castera L, Vergniol J, Foucher J, Le Bail B, Chanteloup E, et al. Prospective comparison of transient elastography, fibrotest, APRI and liver biopsy for the assessment of fibrosis in chronic hepatitis C. Gastroenterology. 2005;128:343.
17. Harada N, Soejima Y, Taketomi A, Yoshizumi T, Ikegami T, Yamashita Y, et al. Assessment of graft fibrosis by transient elastography in patients with recurrent hepatitis C after living donor liver transplantation. Transplantation. 2008;85:69–74.
18. Ziol M, Handra-Luca A, Kettaneh A, Christidis C, Mal F, Kazemi F, de Ledinghen V, et al. Noninvasive assessment of liver fibrosis by measurement of stiffness in patients with chronic hepatitis C. Hepatology. 2005;41:48.
19. Foucher J, Chanteloup E, Vergniol J, Castera L, Le Bail B, Adhoute X, et al. Diagnosis of cirrhosis by transient elastography (FibroScan): a prospective study. Gut. 2006;55:403–8.
20. DeLong ER, DeLong DM, Clarke-Pearson DL. Comparing the area under two or more correlated receiver operating characteristic curves: a nonparametric approach. Biometrics. 1988;44:837–45.
21. Yoshida H, Shiratori Y, Moriyama M, Arakawa Y, Ide T, Sata M, et al. Interferon therapy reduces the risk for hepatocellular carcinoma: national surveillance program of cirrhotic and noncirrhotic patients with chronic hepatitis C in Japan. Ann Intern Med. 1999;131:174–81.
22. Ikeda K, Saitoh S, Suzuki Y, Kobayashi M, Tsubota A, Koida I, et al. Disease progression and hepatocellular carcinogenesis in patients with chronic viral hepatitis: a prospective observation of 2215 patients. J Hepatol. 1998;28:930–8.
23. Ingiliz P, Chhay KP, Munteanu M, Lebray P, Ngo Y, Roulot D, et al. Applicability and variability of liver stiffness measurements according to probe position. World J Gastroenterol. 2009;15:3398–404.
24. Sandrin L, Fourquet B, Hasquenoph JM, Yon S, Fournier C, Mal F, et al. Transient elastography: a new noninvasive method for assessment of hepatic fibrosis. Ultrasound Med Biol. 2003;29:1705–13.

ELSEVIER

INSTITUT PASTEUR

Microbes and Infection 13 (2011) 405–412

www.elsevier.com/locate/micinf

Original article

Intracellular delivery of serum-derived hepatitis C virus

Takasuke Fukuhara [a,b], Hideki Tani [a], Mai Shiokawa [a], Yukinori Goto [a], Takayuki Abe [a], Akinobu Taketomi [b], Ken Shirabe [b], Yoshihiko Maehara [b], Yoshiharu Matsuura [a,*]

[a] *Department of Molecular Virology, Research Institute for Microbial Diseases, Osaka University, 3-1 Yamada-oka, Suita, Osaka 565-0871, Japan*
[b] *Department of Surgery and Science, Graduate School of Medical Sciences, Kyushu University, Fukuoka, Japan*

Received 7 September 2010; accepted 11 January 2011
Available online 22 January 2011

Abstract

A robust and reliable cell culture system for serum-derived HCV (HCVser) has not been established yet because of the presence of neutralizing antibody and tropism for infection. To overcome this obstacle, we employed a lipid-mediated protein intracellular delivery reagent (PIDR) that permits internalization of proteins into cells. Although entry of HCVcc was not enhanced by the treatment with PIDR, entry of HCVser into hepatoma cell lines (Huh7 and HepG2) and immortalized primary hepatocytes (Hc and HuS/E2) was significantly enhanced by the PIDR treatment. The entry of HCVser into Huh7 cells in the presence of PIDR was resistant to the neutralization by an anti-hCD81 antibody, suggesting that PIDR is capable of internalizing HCVser in a receptor-independent manner. Interestingly, the PIDR-mediated entry of HCVser and HCVcc was enhanced by the addition of sera from chronic hepatitis C patients but not from healthy donors. In addition, neutralization of HCVcc infection by anti-E2 antibody was canceled by the treatment with PIDR. In conclusion, the PIDR is a valuable tool to get over the obstacle of neutralizing antibodies to internalize HCV into cells and might be useful for the establishment of *in vitro* propagation HCVser.

Keywords: Hepatitis C virus; Protein intracellular delivery; Serum-derived virus

1. Introduction

More than 170 million individuals worldwide are infected with hepatitis C virus (HCV), and hepatic steatosis, cirrhosis and hepatocellular carcinoma (HCC) induced by HCV infection are life-threatening [1]. Although combined-therapy with peg-interferon (IFN) and ribavirin has achieved a sustained virological response in 50% of individuals infected with HCV genotype 1 [2], a more effective therapeutic modality for HCV infection is needed [3]. To this end, further detailed analyses of HCV are needed in order to clarify not only the viral life cycle but also the pathogenesis. Although cell culture systems for HCV (HCVcc) have been established based on the JFH-1 strain isolated from a fulminant hepatitis C patient [4], such systems were unable to establish chronic infection in chimpanzees [4] or to induce cell damage and inflammation in chimeric mice xenotransplanted with human hepatocytes [5], and therefore establishment of a robust cell culture system capable of propagating serum-derived HCV (HCVser) from hepatitis C patients is required.

Although previous reports suggested a partial replication of HCVser in the primary hepatocytes (PHH) freshly isolated from human liver [6], the level of viral RNA replication was low and reconfirmation of the viral propagation was not achieved due to the difficulty of providing a stable supply of the PHH. Recently, it was shown that a three-dimensional culture system of immortalized PHH was capable of propagating the HCVser from chronic hepatitis C patients [7,8]. HCVser in the patients was slightly amplified in these culture systems, but the levels of viral RNA replication were far lower than those of HCVcc in Huh7-derived adaptive cell lines. Part of the difficulty in establishing a cell culture system for HCVser might be attributable to: i) the

Abbreviations: HCV, hepatitis C virus; IFN, interferon; PHH, primary human hepatocyte; PIDR, protein intracellular delivery reagent; PCR, polymerase chain reaction; VSV, vesicular stomatitis virus.

* Corresponding author. Fax: +81 6 6879 8269.
E-mail address: matsuura@biken.osaka-u.ac.jp (Y. Matsuura).

1286-4579/$ - see front matter © 2011 Institut Pasteur. Published by Elsevier Masson SAS. All rights reserved.
doi:10.1016/j.micinf.2011.01.005

existence of high titers of neutralizing antibodies in the sera of hepatitis C patients [9]; ii) the heterogeneity of HCV particles (quasispecies), which exhibit different cell tropisms for infection and replication [10]; and iii) the inconsistent expression of the putative receptors for HCV entry, including CD81, SR-BI, claudin-1 and occludin [11]. It may be necessary to overcome these obstacles before a robust and reliable *in vitro* cell culture system can be established for HCVser.

Polybrene has been used for the efficient infection of retrovirus [12], and spinoculation has also been employed to accelerate the entry of various viruses, including retrovirus [13] and murine coronavirus [14]. Entry of HCVcc into not only the permissive cell line Huh7.5.1 but also the non-permissive cell line PLC/PRF/5 has been shown to be enhanced by spinoculation [15,16]. In this study, we examined the effects of these accelerating procedures for entry of HCVser and found that a cationic amphiphilic-based lipid-mediated protein intracellular delivery reagent (PIDR) [17] exhibited a potent enhancement of entry of HCVser. Our data suggest that PIDR allows complex formation with viral particles via both electrostatic and hydrophobic interactions and enhances internalization of the HCVser into cells in a receptor-independent manner.

2. Materials and methods

2.1. Sera

Sera from chronic hepatitis C patients and a cured patient possessing the anti-HCV antibodies were obtained at the Kyushu University Hospital after obtaining full informed consent from all patients. Seven serum samples from hepatitis C patients, including two window-period serum samples without any detectable anti-HCV antibodies, were obtained from the Benesis Corporation (Osaka, Japan). Human sera from healthy donors were obtained from Sigma–Aldrich Inc. (St. Louis, MO). Sera from healthy donors, chronic hepatitis patients and acute hepatitis patients were designated HDS, CHS, and AHS, respectively. The HCV-RNA titers of CHS and AHS were 7.15 ± 0.34 (range: 6.6–7.5) and 8.20 ± 0.14 (range: 8.1–8.3), respectively. The genotypes of HCV in these sera were 1a (7 patients) and 1b (11 patients).

2.2. Human liver cell lines and preparation of HCVcc

HepG2 and HEK-293T cell lines were obtained from the American Type Culture Collection (Rockville, MD). The Huh7OK1 cell line exhibits an efficient propagation of HCVcc as described previously [18]. The HepCD81 cell line stably expressing human CD81 was established as described previously [19]. HuS-E/2 was kindly provided by M. Hijikata, Kyoto University [20]. Hc (an immortalized human liver cell line) was purchased from the Applied Cell Biology Research Institute (Kirkland, WA). These cell lines were cultured in Dulbecco's modified Eagle's medium (DMEM) (Sigma) containing 10% fetal bovine serum (FBS). The *in vitro* transcribed RNA of the JFH-1 strain of HCV was introduced into Huh7OK1 cells [21] and culture supernatants were collected at 7 days post-transfection and used as HCVcc. The infectivity of HCVcc was determined by focus forming assay as previously described [19].

2.3. Transfection of plasmids and intracellular delivery of proteins

The plasmids were transfected into cells by liposome-mediated transfection using *Trans*IT-LT1 (Mirus, Madison, WI). The proteins were introduced into cells by PIDR (PULSin; Polyplus-transfection Inc., New York, NY) according to the manufacturer's protocol. FITC-conjugated mouse IgG antibody (Invitrogen Molecular Probes, Eugene, OR) or recombinant phycoerythrin (PE; Polyplus-transfection Inc.) was introduced into cells by the PIDR as a positive control.

2.4. Quantitative reverse-transcription polymerase chain reaction (qRT-PCR)

Total RNA was prepared from cells using an RNeasy mini kit (Qiagen, Tokyo, Japan). The synthesis of first-strand cDNA and qRT-PCR was performed using TaqMan EZ RT-PCR Core Reagents and ABI Prism 7000 system (Applied Biosystems Japan, Tokyo, Japan) according to the manufacturer's protocol. The primers for Taqman PCR were designed in a non-coding region as previously reported [22].

2.5. Infection of HCVser and HCVcc by spinoculation, polybrene and PIDR

Cells were seeded at 1×10^5 cells/well in a 48-well plate and cultured for 24 h. For spinoculation, 2 μl of HCV-positive serum or HCVcc at a multiplicity of infection (MOI) of 0.05 were inoculated into cells and immediately centrifuged at 500× *g* for 120 min at room temperature. For infection of HCV by polybrene and PIDR, 2 μg of polybrene or 1.5 μl of PIDR were incubated with HCV-positive serum or HCVcc diluted in 20 μl of phosphate-buffered saline (PBS) for 15 min at room temperature to allow complex formation [12]. Cells were trypsinized at 24 h post-inoculation, seeded in a 48-well plate to remove non-specific binding of HCV, and cultured for several days.

2.6. Production and infection of pseudotype vesicular stomatitis virus (VSV)

Pseudotype VSVs were generated as described previously [19]. The pseudotype VSVs, VSVpv/GFP and VSVpv/luc, bore the VSVG protein on the virion surface and replaced the G envelope gene with the green fluorescent protein (GFP) and luciferase genes, respectively. Pseudotype VSV bearing HCV E1 and E2 glycoproteins (HCVpv) was prepared as described previously [19]. These pseudotype viruses were inoculated into Huh7OK1 cells in the presence or absence of PIDR together with or without anti-VSVG polyclonal antibody (ab34774; Abcam Inc., Cambridge, MA) or CHS, and infectivity was determined at 24 h post-infection by the expression of GFP or luciferase activity after treatment with a passive lysis buffer (Promega Co., Madison, WI).

2.7. Inhibition of HCVcc and HCVser infection by the treatment with antibody against human CD81 and anti-E2 antibody (AP-33)

To determine the involvement of human CD81 in the intracellular delivery of HCV by PIDR, Huh7OK1 cells were pre-treated with 5 μg/ml of anti-human CD81 monoclonal antibody (JS-81; BD Biosciences Pharmingen, Mountain View, CA) for 1 h at 37 °C and then inoculated with HCVcc or HCVser in the presence of PIDR. Anti-E2 monoclonal antibody (AP-33) was kindly provided by A.H. Patel, University of Glasgow [23]. AP-33 was pre-mixed with HCVcc for 1 h with or without PIDR and then cells were incubated with this mixture and cultured for several days.

3. Results

3.1. Effect of spinoculation and polybrene on the entry of HCVser and HCVcc

First, we examined the effect of spinoculation on the entry of HCVser or HCVcc. Intracellular HCV-RNA titers of Huh7OK1 cells upon infection of HCVser and HCVcc with or without spinoculation at 24 h post-infection were determined (Data not shown). Although entry of HCVcc into Huh7OK1 cells was 10-fold increased by the spinoculation, no effect was observed in the entry of HCVser. Next, we examined the effect of polybrene on the entry of HCVser and HCVcc into Huh7OK1 cells. Although polybrene induced a slight increase of the entry of HCVcc, no significant effect on the entry of HCVser was observed intracellularly at 24 h post-infection (Data not shown). These results indicated that neither spinoculation nor polybrene induced an enhancement of the entry of HCVser.

3.2. Internalization of viral particles by PIDR

To determine the efficacy of intracellular delivery of proteins by PIDR, FITC-conjugated mouse IgG and recombinant PE were introduced into Huh7OK1 cells by PIDR. Both FITC-conjugated IgG and PE were efficiently internalized into Huh7OK1 cells by the treatment with PIDR but not by the lipofection (Fig. 1A). Next, to determine the receptor-independent entry of viral particles into cells by the PIDR, the expression of GFP upon infection of a pseudotype VSV lacking VSVG (VSVΔGpv/GFP) into Huh7OK1 cells was examined. Although VSVΔGpv/GFP lost infectivity due to a lack of the G glycoprotein, the addition of PIDR facilitated entry of the particles (Fig. 1A). To further examine the effect of the presence of neutralization antibody on the delivery of viral particles by PIDR, the expression of GFP upon transduction of VSVpv/GFP into Huh7OK1 cells in the presence of neutralization antibody and PIDR was examined. Although VSVpv/GFP exhibited a high infectivity to Huh7OK1 cells and the infection was completely neutralized by the anti-VSVG antibody, treatment with PIDR partially recovered the infectivity of VSVpv/GFP neutralized by the antibody (Fig. 1B). Similar results were confirmed by using VSVΔGpv/luc and VSVpv/luc carrying the luciferase gene as a reporter (Fig. 1C). These results indicate that PIDR is a useful tool to facilitate the entry of viral particles into target cells, irrespective of the authenticity of the envelope proteins of the particles or the presence of the neutralizing antibodies.

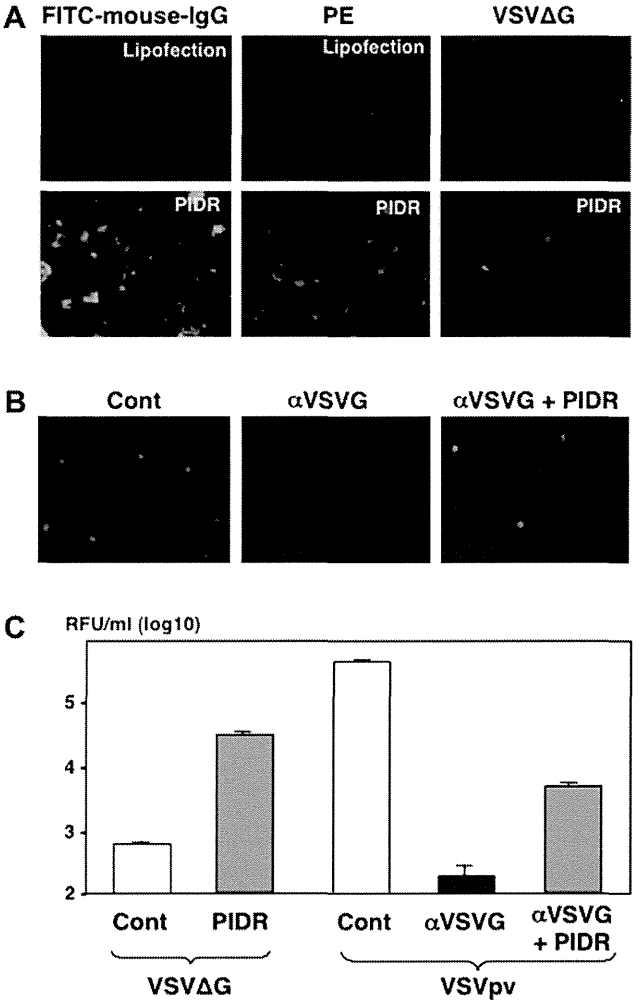

Fig. 1. Characterization of the intracellular delivery of proteins and viral particles by PIDR. (A) FITC-conjugated mouse IgG (left panels) or recombinant PE (center panels) was introduced into Huh7OK1 cells by the treatment with PIDR or a lipofection reagent. The expression of GFP upon infection of a pseudotype VSV lacking VSVG (VSVΔGpv/GFP) into Huh7OK1 cells in the presence (lower panel) and absence (upper panel) of PIDR was examined (right panels). (B) The effect of the presence of neutralization antibody on the delivery of viral particles by PIDR. Expression of GFP upon transduction of a VSVpv/GFP into Huh7OK1 cells in the presence of neutralization antibody and PIDR was examined. (C) The receptor-independent entry of viral particles was confirmed by using VSVΔGpv/luc and VSVpv/luc carrying the luciferase gene as a reporter.

3.3. Effect of PIDR on the infection with HCVcc

To determine the effect of PIDR on the infection of HCV, HCVcc was inoculated into Huh7OK1 cells at an MOI of 0.05 in the presence or absence of PIDR and intracellular viral

RNA was measured every 24 h. No significant difference in the infection of HCVcc was observed by the addition of PIDR (Fig. 2A). Next, to mimic the infection of HCV in the presence of neutralization antibodies, HCVcc was mixed with CHS and inoculated into Huh7OK1 cells. Although infection of HCVcc into Huh7OK1 was completely neutralized by the incubation with CHS, addition of PIDR recovered the infectivity of HCVcc (Fig. 2B). Furthermore, to confirm the effect of PIDR on the internalization of HCVcc interacting with neutralizing antibody, HCVcc was pre-incubated with AP-33 and inoculated into Huh7OK1 cells. Although infection of HCVcc was neutralized by the treatment with AP-33 in a dose-dependent manner, the neutralization by AP-33 was canceled by the treatment with PIDR (Fig. 2C). These results suggest that PIDR has the ability to internalize HCVcc even in the presence of neutralizing antibodies.

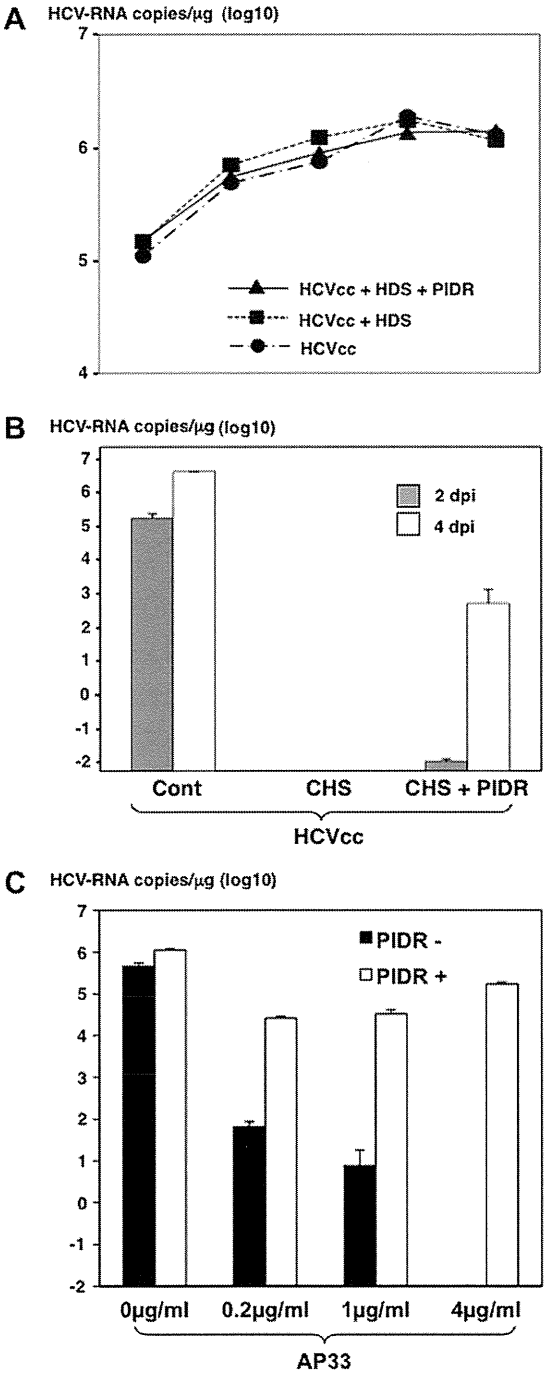

Fig. 2. Effect of PIDR on the infection with HCVcc. (A) HCVcc was inoculated into Huh7OK1 cells at an MOI of 0.05 in the presence or absence of healthy donor sera (HDS) and PIDR and intracellular viral RNA was measured every 24 h (B) HCVcc was mixed with sera from chronic hepatitis C patients (CHS) or/and PIDR and inoculated into Huh7OK1 cells. (C) HCVcc was premixed with anti-E2 monoclonal antibody (AP-33) and inoculated into Huh7OK1 cells in the presence or absence of PIDR.

3.4. Effect of PIDR on the infection of HCVser

The efficient neutralizing activities of HCV infection in CHS were comfirmed by a neutralization assay using pseudotype viruses. Infection of HCVpv bearing HCV E1 and E2 proteins but not of VSVpv bearing VSVG protein was significantly neutralized by the CHS (Fig. 3A). Next, to determine the effect of PIDR on the entry of HCVser in the presence of neutralizing antibodies, HCVser and CHS possessing the neutralizing antibodies against HCV were inoculated into Huh7OK1 cells with or without incubation with PIDR. Huh7OK1 cells inoculated with CHS pre-incubated with PIDR exhibited significantly higher HCV-RNA titers at 24 h post-infection than those without the treatment (Fig. 3B). Furthermore, to determine the amount of HCV internalized into cells, Huh7OK1 cells inoculated with CHS treated with PIDR were trypsinized and reseeded into a new culture plate at 24 h post-infection. HCV-RNA was detected in cells inoculated CHS pre-incubated with PIDR but not in those without PIDR treatment at 24 h after reseeding (Fig. 3C). These results indicate that treatment with PIDR permits HCVser to internalize into target cells even in the presence of neutralizing antibodies.

3.5. Neutralizing antibodies in sera from chronic hepatitis C patients enhance PIDR-mediated entry of HCV

No reduction of infectivity of HCVpv and VSVpv was observed by the incubation with AHS, suggesting that AHS possesses no detectable neutralizing antibodies to HCV (Fig. 4A). To examine the effect of neutralizing antibody on the intracellular delivery of HCVser by PIDR, AHS was incubated with the CHS carrying neutralization antibodies but no infectious HCV obtained from patients cured by the interferon therapy in the presence or absence of PIDR and inoculated into Huh7OK1 cells. Internalization of HCV in AHS was increased two-fold by the treatment with PIDR. However, intracellular viral RNA titer was slightly decreased by the incubation with CHS in the absence of PIDR, probably due to the neutralization by the antibodies, and addition of PIDR resulted in a three-fold enhancement of the entry of HCV in AHS in the presence of CHS compared with that in the absence of CHS (Fig. 4B). Next, Huh7OK1 cells were inoculated with HCVcc at an MOI of 0.05 after incubation with 0.4–40 μl/ml of HCV-negative CHS in the presence or absence of PIDR. Although infection of HCVcc was

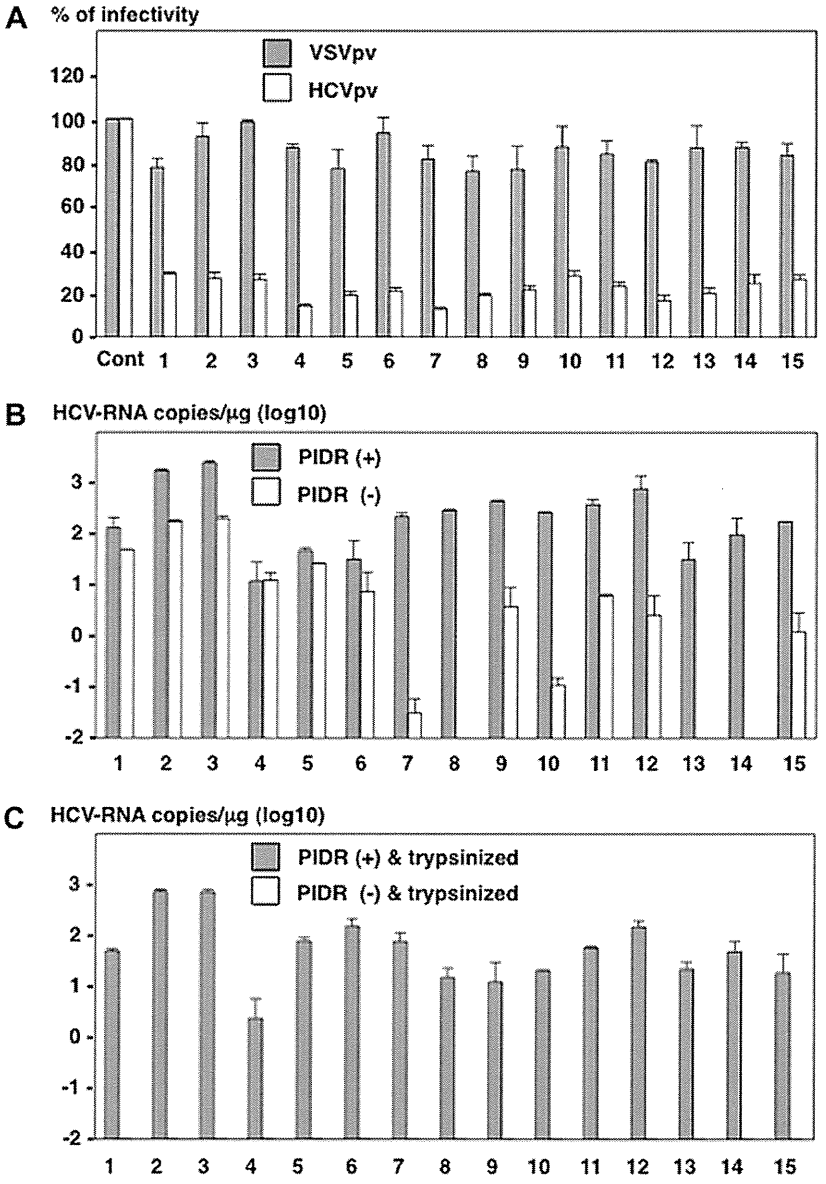

Fig. 3. Effect of PIDR on the infection with HCVser. (A) The neutralizing effect of antibodies in the CHS was determined by a neutralization assay using the pseudotype viruses. White and gray bars indicated VSVpv and HCVpv, respectively. (B) The effect of PIDR on the entry of HCVser in the CHS into Huh7OK1 cells. HCV-RNA titers in cells 24 h post-inoculation with HCVser in the presence and absence of PIDR are indicated by gray and white bars, respectively. (C) To determine the internalization of HCVser into Huh7OK1 cells, cells inoculated with the CHS in the presence (gray bar) or absence (white bars) of PIDR were trypsinized and reseeded into a new culture plate at 24 h post-infection, and HCV-RNA titers in the cells were determined at 24 h post-inoculation.

neutralized by CHS in a dose-dependent manner, addition of PIDR enhanced the infection of HCVcc in the presence of CHS in a dose-dependent manner (Fig. 4C). These results indicate that PIDR facilitates entry of HCVser in the presence of neutralizing antibody.

3.6. Human CD81-independent entry of HCVser by PIDR

Next, to determine the involvement of human CD81 (hCD81), a major receptor candidate for HCV [24], on the PIDR-mediated entry of HCVser, Huh7OK1 cells were pre-treated with anti-hCD81 antibody and inoculated with HCVser treated with PIDR. Although pretreatment with anti-hCD81 antibody resulted in a significant reduction in the entry of HCVser, treatment with PIDR enhanced the entry of HCVser irrespective of the presence of the anti-human CD81antibody (Fig. 5A). In addition, although entry of HCVser into HepG2 and HepCD81 cells was low and independent of the expression of hCD81, treatment with PIDR enhanced the entry of HCVser irrespective of the expression of human CD81 (Fig. 5B). These results suggest that the PIDR-mediated entry of HCVser is independent of the expression of hCD81 and is effective for the entry of HCVser into various cell lines other than Huh7-derived cell lines.

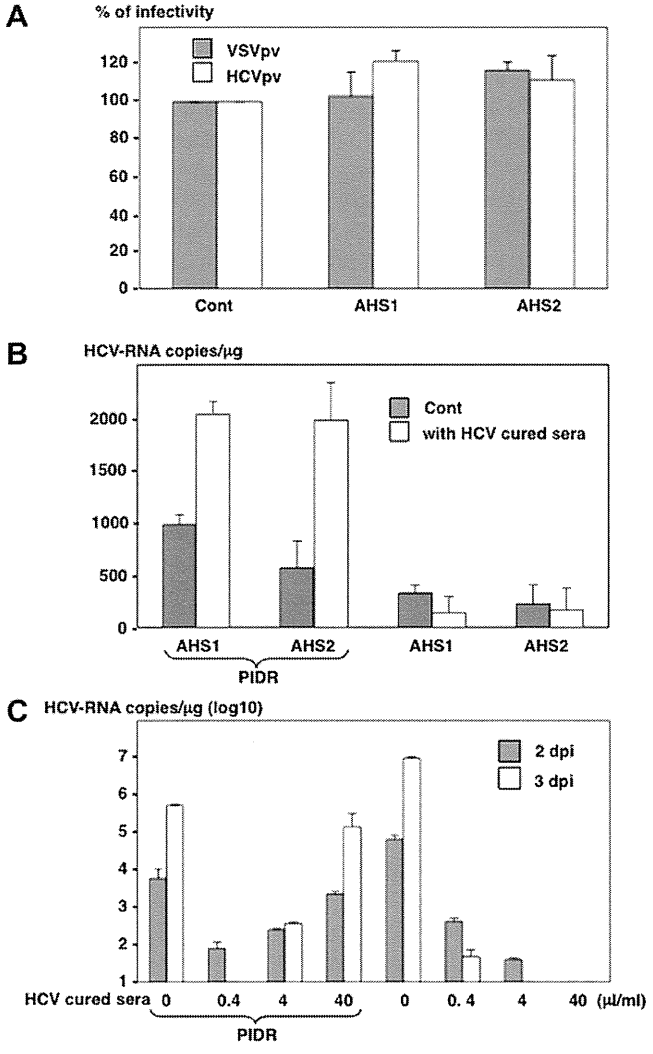

Fig. 4. Neutralizing antibodies in the CHS enhanced the PIDR-mediated entry of HCV. (A) The absence of neutralizing antibodies in the sera from acute hepatitis C patients (AHS) was determined by a neutralization assay using the HCVpv (white bars) and VSVpv (gray bar). (B) The effect of PIDR on the entry of HCVser into Huh7OK1 cells in the presence of neutralizing antibodies. The AHS were incubated with the CHS carrying neutralization antibodies but no infectious HCV obtained from patients cured by the IFN therapy (white bars) or HDS (gray bar) in the presence (left) or absence (right) of PIDR and inoculated into Huh7OK1 cells. The HCV-RNA titers in cells were determined at 24 h post-inoculation. (C). The effect of neutralizing antibodies on the PIDR-mediated infection of HCVcc. Huh7OK1 cells were inoculated with HCVcc at an MOI of 0.05 after incubation with 0.4–40 μl/ml of HCV-negative CHS in the presence (left) or absence (right) of PIDR. Gray and white bars indicate the HCV-RNA titers at 2 and 3 days after infection, respectively.

3.7. Effect of PIDR on the entry of HCVser into immortalized human hepatocytes

Recently, Aly et al. reported that immortalized human hepatocytes, HuS/E2 cells, exhibited a high susceptibility to the infection with HCVser [7]. Therefore, we examined the effect of PIDR on the entry of HCVser into immortalized human hepatocytes, including Hc and HuS/E2 cells. The addition of PIDR enhanced the entry of HCVser into both Hc and HuS/E2 cells

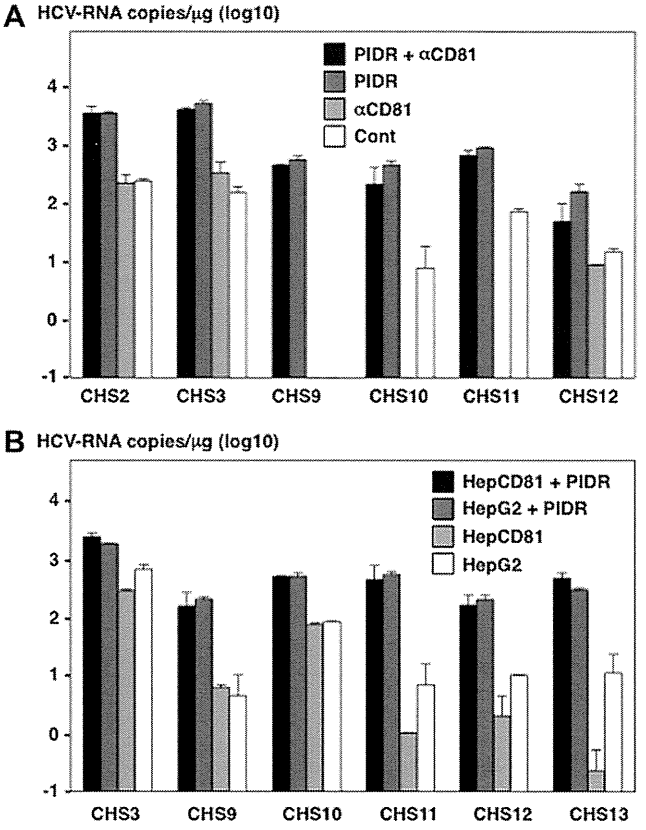

Fig. 5. Human CD81-independent entry of HCVser by PIDR. (A) The effect of anti-hCD81 antibody on the entry of HCVser into Huh7OK1 cells in the presence or absence of PIDR. (B) The effect of PIDR on the entry of HCVser into HepG2 and HepCD81 cells. HCV-RNA titers in cells were determined at 24 h post-inoculation.

(Fig. 6A and B). These results indicate that PIDR has the potential to enhance the entry of HCVser into not only cancer cell lines but also immortalized hepatocytes. Next, to evaluate the long-term effect of PIDR treatment on the infectivity of HCVser, Hc cells inoculated with CHS pre-incubated with PIDR were cultured for a long period. HCV-RNA could be detected at 10, 15 and 20 days after PIDR-mediated infection (Fig. 6C). However, significant elevations of HCV-RNA titers were not seen (Data not shown).

4. Discussion

In this study, we examined the efficiency of intracellular deliveries of HCVser by using spinoculation, polybrene and PIDR and found that the PIDR exhibited the highest efficacy on the entry of HCVser into target cells. Especially, trypsinization and reseeding of cells dramatically reduced HCV-RNA levels in groups that were not treated with PIDR as compared to those were treated with PIDR (Fig. 3B and C), and PIDR treatment dramatically increased the internalization of HCVcc treated with CHS or AP-33 at 2 and 4 days after infection (Fig. 2B and C). These results suggest that PIDR is feasible to deliver HCV/CHS complexes into target cells that allow productive infection. In addition, PIDR facilitated the entry of

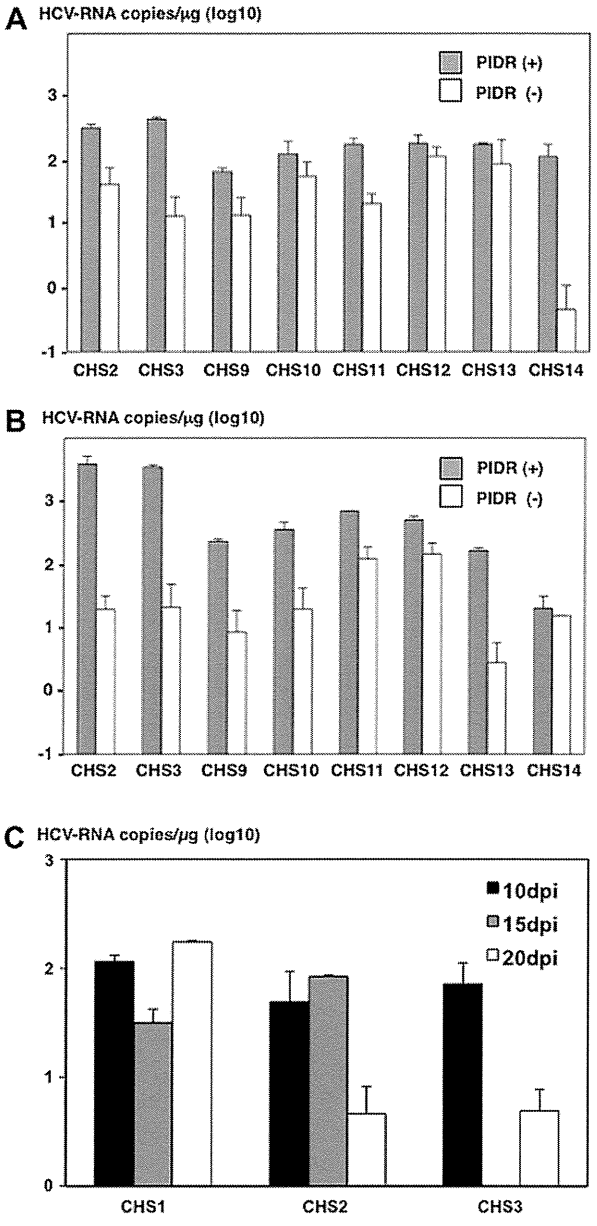

Fig. 6. Effect of PIDR on the entry of HCVser into immortalized human hepatocytes. The effect of PIDR on the entry of HCVser into immortalized human hepatocytes, such as Hc (A) and HuS/E2 (B) cells. The HCV-RNA titers in cells were determined at 24 h post-inoculation. (C) HCV-RNA titers in Hc cells inoculated with HCVser were evaluated at 10, 15 and 20 days after PIDR-mediated infection.

HCVser into the hepatoma cell lines and immortalized human hepatocytes in an hCD81-independent manner. Furthermore, we demonstrated that the intracellular delivery of HCVser by PIDR was enhanced by the addition of anti-HCV antibodies in sera from chronic hepatitis C patients, suggesting that PIDR is an effective reagent for the intracellular delivery of HCVser into the target cells in a receptor-independent manner.

Although direct evidence of enhancement of the adsorption and penetration by the application of spinoculation and polybrene has not been demonstrated yet, sedimentation of the virus particles to the cell surface by the spinoculation and electrostatic interactions between viral particles and cells by the charged polybrene are suggested to overcome the first barrier between virus particles and cells [12–14]. PIDR is a cationic amphiphilic-based protein delivery reagent that forms a complex with proteins through electrostatic and hydrophobic interactions [17]. The complexes of protein molecules and PIDR have been shown to interact with heparan sulfate proteoglycans on the cell surface, and then to be internalized through endocytosis, after which the protein molecules are released from the complexes into the cytoplasm [17], suggesting that PIDR is capable of enhancing not only adsorption but also penetration of HCVser.

Although HCVser are composed of heterogenous viral populations and a large fraction of the viral particles was associated with lipoproteins or neutralizing antibodies [25], these particles are capable of invading into human hepatocytes and establishing a persistent infection *in vivo* [1]. Therefore, it is feasible to speculate that some host factors are involved in the entry of HCVser into hepatocytes *in vivo*. Recently, Stamataki et al. [26] suggested that peripheral blood B lymphocytes participate as a reservoir for HCV for persistent infection and as a vehicle for transinfection to hepatocytes. Although the precise mechanisms of the entry of HCV have not been clarified yet, PIDR is an efficient modality to overcome the obstacles to the entry of HCV.

Recent studies have revealed that at least four cellular molecules play crucial roles in the infection of HCV into hepatocytes *in vitro*: hCD81, scavenger receptor class B type I (SR-BI) [27], and tight junction proteins claudin-1 [28] and occludin [11]. In this study, the entry of HCVser by the treatment with PIDR was shown to be independent from hCD81. Although the involvement of receptor candidates other than hCD81 was not examined in this study, PIDR was shown to enhance the entry of HCVser in cell lines including Huh7, HepG2, HepCD81, Hc and HuS/E2, suggesting that PIDR is capable of enhancing the entry of HCV through a pathway independent from the expression of these receptor candidates.

Previous studies have indicated that HCV infects not only hepatocytes but also lymphoid tissues and peripheral blood mononuclear cells [29], and that the quasispecies nature of viral particles was different among tissues infected with HCV [10]. Furthermore, it was shown that the *in vitro* transcribed JFH-1 RNA used for the recovery of infectious particles contained 2.21×10^{11} copies/μg [30], which is much higher than the amount of viral RNA detected in the patient's sera. The variety of cell tropisms depending on the quasispecies of HCV particles, a low viral load in sera co-existing with neutralization antibodies, and the lack of identified co-factors including functional environment of the liver might be the major obstacles to establishing cell culture systems for the propagation of HCVser. Several approaches have been taken for the establishment of an *in vitro* cell culture system of HCV, including the culture of human liver cells in a three-dimensional radial-flow bioreactor [31], the three-dimensional culture of immortalized primary hepatocytes [7], and the micropatterned culture of primary hepatocytes [8]. These innovative approaches to the cell culture of liver cells, in combination with PIDR which is able to overcome the first barrier of HCV propagation might

contribute to a breakthrough in the establishment of a robust cell culture system of HCVser.

In this study, we demonstrated that PIDR is able to internalize HCV in a receptor-independent manner and provides a clue toward the development of a cell culture system of HCVser in the presence of neutralization antibodies. PIDR may also be useful for the study of viruses that are difficult to internalize into cells due to their low viral titers or the presence of neutralizing antibodies.

Acknowledgments

We thank H. Murase for secretarial work.

This research was supported in part by grants-in-aid from the Ministry of Health, Labor, and Welfare, and the Ministry of Education, Culture, Sports, Science, and Technology, Japan.

References

[1] L.-B. Seeff, Natural history of chronic hepatitis C, Hepatology 36 (2002) S35–S46.

[2] M.-P. Manns, J.-G. McHutchison, S.-C. Gordon, V.-K. Rustgi, M. Shiffman, R. Reindollar, Z.-D. Goodman, K. Koury, M. Ling, J.-K. Albrecht, Peginterferon alfa-2b plus ribavirin compared with interferon alfa-2b plus ribavirin for initial treatment of chronic hepatitis C: a randomised trial, Lancet 358 (2001) 958–965.

[3] J.-M. Pawlotsky, S. Chevaliez, J.-G. McHutchison, The hepatitis C virus life cycle as a target for new antiviral therapies, Gastroenterology 132 (2007) 1979–1998.

[4] T. Wakita, T. Pietschmann, T. Kato, T. Date, M. Miyamoto, Z. Zhao, K. Murthy, A. Habermann, H.-G. Krausslich, M. Mizokami, R. Bartenschlager, T. Jake-Liang, Production of infectious hepatitis C virus in tissue culture from a cloned viral genome, Nat. Med. 11 (2005) 791–796.

[5] N. Hiraga, M. Imamura, M. Tsuge, C. Noguchi, S. Takahashi, E. Iwao, Y. Fujimoto, H. Abe, T. Maekawa, H. Ochi, C. Tateno, K. Yoshizawa, A. Sakai, Y. Sakai, M. Honda, S. Kaneko, T. Wakita, K. Chayama, Infection of human hepatocyte chimeric mouse with genetically engineered hepatitis C virus and its susceptibility to interferon, FEBS Lett. 581 (2007) 1983–1987.

[6] S. Molina, V. Castet, L. Pichard-Garcia, C. Wychowski, E. Meurs, J.-M. Pascussi, C. Sureau, J.-M. Fabre, A. SaCunha, D. Larrey, J. Dubuisson, J. Coste, J. McKeating, P. Maurel, C. Fournier-Wirth, Serum-derived hepatitis C virus infection of primary human hepatocytes is tetraspanin CD81 dependent, J. Virol. 82 (2008) 569–574.

[7] H.-H. Aly, Y. Qi, K. Atsuzawa, N. Usuda, Y. Takada, M. Mizokami, K. Shimotohno, M. Hijikata, Strain-dependent viral dynamics and virus-cell interactions in a novel in vitro system supporting the life cycle of blood-borne hepatitis C virus, Hepatology 50 (2009) 689–696.

[8] A. Ploss, S.-R. Khetani, C.-T. Jones, A.-J. Syder, K. Trehan, V.-A. Gaysinskaya, K. Mu, K. Ritola, C.-M. Rice, S.-N. Bhatia, Persistent hepatitis C virus infection in microscale primary human hepatocyte cultures, Proc. Natl. Acad. Sci. U. S. A 107 (2010) 3141–3145.

[9] D.-R. Burton, Antibodies, viruses and vaccines, Nat. Rev. Immunol. 2 (2002) 706–713.

[10] R. Sobesky, C. Feray, F. Rimlinger, N. Derian, A. Dos Santos, A.-M. Roque-Afonso, D. Samuel, C. Brechot, V. Thiers, Distinct hepatitis C virus core and F protein quasispecies in tumoral and nontumoral hepatocytes isolated via microdissection, Hepatology 46 (2007) 1704–1712.

[11] A. Ploss, M.-J. Evans, V.-A. Gaysinskaya, M. Panis, H. You, Y.-P. de Jong, C.-M. Rice, Human occludin is a hepatitis C virus entry factor required for infection of mouse cells, Nature 457 (2009) 882–886.

[12] N. Landazuri, J.-M. Le Doux, Complexation of retroviruses with charged polymers enhances gene transfer by increasing the rate that viruses are delivered to cells, J. Gene Med. 6 (2004) 1304–1319.

[13] U. O'Doherty, W.-J. Swiggard, M.-H. Malim, Human immunodeficiency virus type 1 spinoculation enhances infection through virus binding, J. Virol. 74 (2000) 10074–10080.

[14] R. Watanabe, S. Matsuyama, F. Taguchi, Receptor-independent infection of murine coronavirus: analysis by spinoculation, J. Virol. 80 (2006) 4901–4908.

[15] L. Ye, X. Wang, S. Wang, G. Luo, Y. Wang, H. Liang, W. Ho, Centrifugal enhancement of hepatitis C virus infection of human hepatocytes, J. Virol. Methods 148 (2008) 161–165.

[16] I. Benedicto, F. Molina-Jimenez, B. Bartosch, F.-L. Cosset, D. Lavillette, J. Prieto, R. Moreno-Otero, A. Valenzuela-Fernandez, R. Aldabe, M. Lopez-Cabrera, The tight junction-associated protein occludin is required for a postbinding step in hepatitis C virus entry and infection, J. Virol. 83 (2009) 8012–8020.

[17] C.-O. Weill, S. Biri, A. Adib, P. Erbacher, A practical approach for intracellular protein delivery, Cytotechnology 56 (2008) 41–48.

[18] T. Okamoto, H. Omori, Y. Kaname, T. Abe, Y. Nishimura, T. Suzuki, T. Miyamura, T. Yoshimori, K. Moriishi, Y. Matsuura, A single-amino-acid mutation in hepatitis C virus NS5A disrupting FKBP8 interaction impairs viral replication, J. Virol. 82 (2008) 3480–3489.

[19] H. Tani, Y. Komoda, E. Matsuo, K. Suzuki, I. Hamamoto, T. Yamashita, K. Moriishi, K. Fujiyama, T. Kanto, N. Hayashi, A. Owsianka, A.-H. Patel, M.-H. Whitt, Y. Matsuura, Replication-competent recombinant vesicular stomatitis virus encoding hepatitis C virus envelope proteins, J. Virol. 81 (2007) 8601–8612.

[20] H.-H. Aly, K. Watashi, M. Hijikata, H. Kaneko, Y. Takada, H. Egawa, S. Uemoto, K. Shimotohno, Serum-derived hepatitis C virus infectivity in interferon regulatory factor-7-suppressed human primary hepatocytes, J. Hepatol. 46 (2007) 26–36.

[21] J. Zhong, P. Gastaminza, G. Cheng, S. Kapadia, T. Kato, D.-R. Burton, S.-F. Wieland, S.-L. Uprichard, T. Wakita, F.-V. Chisari, Robust hepatitis C virus infection in vitro, Proc. Natl. Acad. Sci. U. S. A 102 (2005) 9294–9299.

[22] T. Morris, B. Robertson, M. Gallagher, Rapid reverse transcription-PCR detection of hepatitis C virus RNA in serum by using the TaqMan fluorogenic detection system, J. Clin. Microbiol. 34 (1996) 2933–2936.

[23] R.F. Clayton, A. Owsianska, J. Aitken, S. Graham, D. Bhella, A.H. Patel, Analysis of antigenicity and topology of E2 glycoprotein present on recombinant hepatitis C virus-like particles, J. Virol. 76 (2002) 7672–7682.

[24] P. Pileri, Y. Uematsu, S. Campagnoli, G. Galli, F. Falugi, R. Petracca, A.-J. Weiner, M. Houghton, D. Rosa, G. Grandi, S. Abrignani, Binding of hepatitis C virus to CD81, Science 282 (1998) 938–941.

[25] D. Lavillette, Y. Morice, G. Germanidis, P. Donot, A. Soulier, E. Pagkalos, G. Sakellariou, L. Intrator, B. Bartosch, J.-M. Pawlotsky, F.-L. Cosset, Human serum facilitates hepatitis C virus infection, and neutralizing responses inversely correlate with viral replication kinetics at the acute phase of hepatitis C virus infection, J. Virol. 79 (2005) 6023–6034.

[26] Z. Stamataki, C. Shannon-Lowe, J. Shaw, D. Mutimer, A.-B. Rickinson, J. Gordon, D.-H. Adams, P. Balfe, J.-A. McKeating, Hepatitis C virus association with peripheral blood B lymphocytes potentiates viral infection of liver-derived hepatoma cells, Blood 113 (2009) 585–593.

[27] E. Scarselli, H. Ansuini, R. Cerino, R.-M. Roccasecca, S. Acali, G. Filocamo, C. Traboni, A. Nicosia, R. Cortese, A. Vitelli, The human scavenger receptor class B type I is a novel candidate receptor for the hepatitis C virus, EMBO. J. 21 (2002) 5017–5025.

[28] M.-J. Evans, T. von Hahn, D.-M. Tscherne, A.-J. Syder, M. Panis, B. Wolk, T. Hatziioannou, J.-A. McKeating, P.-D. Bieniasz, C.-M. Rice, Claudin-1 is a hepatitis C virus co-receptor required for a late step in entry, Nature 446 (2007) 801–805.

[29] J.-T. Blackard, N. Kemmer, K.-E. Sherman, Extrahepatic replication of HCV: insights into clinical manifestations and biological consequences, Hepatology 44 (2006) 15–22.

[30] T. Kato, T. Date, M. Miyamoto, A. Furusaka, K. Tokushige, M. Mizokami, T. Wakita, Efficient replication of the genotype 2a hepatitis C virus subgenomic replicon, Gastroenterology 125 (2003) 1808–1817.

[31] H. Aizaki, S. Nagamori, M. Matsuda, H. Kawakami, O. Hashimoto, H. Ishiko, M. Kawada, T. Matsuura, S. Hasumura, Y. Matsuura, T. Suzuki, T. Miyamura, Production and release of infectious hepatitis C virus from human liver cell cultures in the three-dimensional radial-flow bioreactor, Virology 314 (2003) 16–25.

Liver INTERNATIONAL
OFFICIAL JOURNAL OF THE INTERNATIONAL ASSOCIATION FOR THE STUDY OF THE LIVER

Liver International ISSN 1478-3223

CLINICAL STUDIES

Clinical significance and potential of hepatic microRNA-122 expression in hepatitis C

Kazutoyo Morita, Akinobu Taketomi, Ken Shirabe, Kenji Umeda, Hiroto Kayashima, Mizuki Ninomiya, Hideaki Uchiyama, Yuji Soejima and Yoshihiko Maehara

Department of Surgery and Science, Graduate School of Medical Sciences, Kyushu University, Fukuoka, Japan

Keywords
hepatitis C virus – liver damage – microRNA-122 – stratified analysis – viral load

Abbreviations
HCC, hepatocellular carcinoma; HCV, hepatitis C virus; IFN, interferon; LDLT, living donor liver transplantation; miR-122, microRNA-122; miRNA, microRNA; qRT-PCR, quantitative reverse transcription polymerase chain reaction; UTR, untranslated region

Correspondence
Kazutoyo Morita, MD, Department of Surgery and Science, Graduate School of Medical Sciences, Kyushu University, 3-1-1 Maidashi, Higashi-ku, Fukuoka 812-8582, Japan
Tel: +81 92 642 5466
Fax: +81 92 642 5482
e-mail: kamorita@surg2.med.kyushu-u.ac.jp

Received 17 December 2009
Accepted 29 November 2010

DOI:10.1111/j.1478-3231.2010.02433.x

Abstract

Background and aims: MicroRNAs are small non-coding RNA molecules that post-transcriptionally regulate gene expression. Liver-specific microRNA-122 (miR-122) has been shown to facilitate the replication of hepatitis C virus (HCV) in human hepatoma cells *in vitro*. However, the clinical significance of hepatic miR-122 on HCV in human body is unclear. *Methods:* Hepatic miR-122 expression was quantified using quantitative reverse-transcription polymerase chain reaction. We investigated the correlation between miR-122 expression and HCV load in liver samples from 185 patients seropositive for HCV antibody, including 151 patients seropositive for HCV RNA, and 31 patients seronegative for HCV RNA. *Results:* Although hepatic miR-122 expression was weakly and positively correlated with the serum HCV load ($\rho = 0.19$, $P < 0.05$), it was not correlated with the hepatic HCV load ($\rho = -0.14$, $P = 0.08$). The absence of a correlation between miR-122 expression and hepatic HCV load was also confirmed after stratification of histopathological liver damage (inflammatory activity grades and fibrosis stages). Furthermore, hepatic miR-122 expression in patients seronegative for HCV RNA was significantly higher than that in patients seropositive for HCV RNA ($P < 0.0001$). The level of hepatic miR-122 expression was inversely correlated with the severity of functional and histopathological liver damage ($P < 0.0001$), serum transaminase levels ($P < 0.0005$). *Conclusions:* Compared with *in vitro* findings, hepatic miR-122 expression is not correlated with HCV load in the human liver. Therefore, miR-122, by itself, is not a critical molecular target for HCV therapy. MiR-122 expression is inversely correlated with both functional and histopathological liver damage.

MicroRNAs (miRNAs) are small non-coding RNAs, approximately 21–22 nucleotides in length, that regulate gene expression through partial or complete complementarity with target messenger RNAs (1–3). MiRNAs are implicated in many biological processes and diverse diseases such as in viral infections and cancers (4–6).

MicroRNA-122 (miR-122) is a liver-specific miRNA accounting for 70% of the total liver miRNA content (7, 8). MiR-122 is reported to facilitate the replication of hepatitis C virus (HCV) in cultured human hepatoma cells stably expressing the HCV replicon (9–13) by binding to the complementary target sequences in the 5′-untranslated region (UTR) of HCV RNA (9, 10, 13). Furthermore, sequestration of miR-122 in hepatoma cells by antisense oligonucleotides decreased HCV replication (9–13) and translation (14). Interferon-beta (IFN-β), a cytokine with potent antiviral activity against HCV, was shown to reduce HCV replication and miR-122 expression in Huh-7 cells, which indicates that the repression of miR-122 might be involved in the antiviral mechanism of IFN-β (15). These *in vitro* reports prompted much interest in the effect of miR-122 on hepatitis C and prompted the expectation that inhibiting hepatic miR-122 may contribute to the novel molecular-targeted therapy of hepatitis C (9–15).

By contrast to the findings *in vitro* from many studies, the clinical impact of hepatic miR-122 on HCV in human body is still unclear. It was recently reported that miR-122 is decreased in the liver of HCV patients if compared to control liver tissue and that the miR-122 level is correlated to the clinical response to peg-IFN-α, but was not correlated with the HCV load, based on a study of 42 patients seropositive for HCV RNA (16). Their study provided a perspective on the role of miRNAs in HCV infection and the antiviral activity of IFN *in vivo*. However, the number of the cases was small and the absence of a correlation between miR-122 and HCV load was shown in 42 cases across wide ranges of inflammation

activity grades and fibrosis stages, which possibly affected the analytic result because of growth of non-hepatocytes and a relative decrease in the number of hepatocytes. At the time of that publication, we had already started a study based including more than four times the number of HCV-infected patients in Japan ($n = 185$) and we have recently completed detailed analyses, including stratification of grades of liver damage to account for the effect of growth of cells other than hepatocytes.

In the present study, we quantified hepatic miR-122 expression in 185 patients seropositive for HCV antibody using quantitative reverse-transcription polymerase chain reaction (qRT-PCR). Then, we evaluated the association between hepatic miR-122 expression and clinical parameters, including serum and hepatic HCV load, functional and histopathological liver damage, serum transaminase levels. The analyses were repeated in two genotypes (genotypes 1 and 2) and after stratification for histopathological liver damage to enhance the reliability of our study.

Materials and methods

Patient characteristics and human liver tissues

Liver specimens were obtained from 204 patients who had undergone hepatic resection or living donor liver transplantation (LDLT) at the Department of Surgery and Science, Kyushu University Hospital (Fukuoka, Japan) between July 2003 and December 2008. This study conformed to the ethical guidelines of the 1975 Declaration of Helsinki. The study protocol was approved by the institutional review board and informed consent was obtained from each patient. This population was divided into two groups, the HCV-infected group and the control group. The HCV-infected group consisted of 185 patients seropositive for the HCV antibody. Of these, 151 patients were seropositive for HCV RNA, 31 patients were seronegative for HCV RNA and serum HCV RNA status was unknown in three patients. Histopathologically, the 185 patients included 161 patients with hepatocellular carcinoma (HCC), 19 patients with hepatitis C cirrhosis without HCC, four patients with hepatocholangiocellular carcinoma and one patient with angiomyolipoma. The control group consisted of 19 patients with a histologically normal liver, including 16 cases of living donors for LDLT and three cases with metastatic liver tumour. Surgically resected liver specimens were snap-frozen and stored at $-80\,^{\circ}C$ until RNA extraction. In the cases of living donors of LDLT, the samples were obtained from an intra-operative biopsy. In the cases with multiple HCCs, the tissue sample from the largest HCC in each case was assayed. In the HCV-infected group ($n = 185$), 139 samples of primary hepatic cancer (135 samples of HCC samples and four samples of hepatocholangiocellular carcinoma) and all 185 non-cancerous liver samples were assayed. In the control group ($n = 19$), all 19 histologically normal liver samples were assayed, but the samples of metastatic liver tumours were not. The clinical characteristics of the patients are shown in Table 1.

RNA isolation

Total RNA containing miRNA was isolated from the frozen liver tissues using mirVana miRNA isolation kit (Ambion, Austin, TX, USA) in accordance with the manufacturer's protocol. Pre-operative serum samples were obtained from 40 cases (35 cases with HCV, five cases with a histologically normal liver). Total RNA was isolated from the 1 ml of serum using ISOGEN-LS (Nippon Gene, Tokyo, Japan) in accordance with the manufacturer's protocol.

Quantitative reverse transcription-polymerase chain reaction for microRNA expression

Hepatic miR-122 expression was quantified using TaqMan® MicroRNA assays (Applied Biosystems, Foster City, CA, USA) in accordance with the manufacturer's protocol. Reverse transcription was performed using 10 ng of the isolated total RNAs from liver tissues and 100 ng of the isolated RNAs from serum samples.

Table 1. Clinical and histopathological characteristics of the patients

Factor	HCV-infected group ($n = 185$)	Control group ($n = 19$)
Sex (male/female)	130/55	14/5
Age (years)	62.3 ± 10.7	41.4 ± 13.7
Viral infection status		
HBs antigen (+/−)	2/183	0/19
HCV antibody (+/−)	185/0	0/19
Serum HCV RNA (+/−/NA)	151/31/3	None
HCV genotype (1/2/NA)	113/31/41	None
Liver function		
Albumin (g/dl)	3.4 ± 0.6	4.3 ± 0.5
Total biliribin (mg/dl)	2.3 ± 4.0	0.8 ± 0.5
Prothrombin time (%)	70.0 ± 20.6	94.1 ± 8.9
Child–Pugh grade (A/B/C)	90/41/54	19/0/0
Non-cancerous liver		Normal liver
Activity (A0/A1/A2/A3)	3/51/110/21	19/0/0/0
Fibrosis (F0/F1/F2/F3/F4)	7/24/15/13/126	19/0/0/0/0
Histopathological hepatic tumor		
Hepatocellular carcinoma	161 (135)*	0
Hepatocholangiocellular carcinoma	4 (4)*	0
Angiomyolipoma	1 (0)*	0
Metastatic liver tumor	0	3 (0)*
None	19	16
Differentiation of hepatic cancer		
Well	12 (5)*	None
Moderate	109 (96)*	None
Poor	44 (38)*	None
Tumour factor		
T1/T2/T3/T4	67/86/12/0 (54/74/11/0)*	None

*Cases (nodules available for the assays).

HBs, hepatitis B surface; HCV, hepatitis C virus; NA, not applicable.

Real-time PCR was performed on an ABI Prism 7700 Sequence Detection System (Applied Biosystems). The miR-122 expression in the samples was quantified by the relative standard curve method using a control sample (histopathologically normal liver sample from a patient with metastatic liver tumour) and normalized by RNU6B expression. After normalization, the expression values were calculated relative to the control sample (the liver sample or serum sample from the patient with metastatic liver tumour).

Quantification of serum and hepatic HCV load

Quantification of pre-operative serum HCV RNA load (Log IU/mL) and/or the pre-operative HCV genotyping was performed by SRL Inc. Fukuoka Laboratory (Fukuoka, Japan) using a COBAS Amplicor HCV Monitor version 2.0 or COBAS Taqman® HCV assays (Roche Diagnostics, Mannheim, Germany). Hepatic HCV RNA load (log copies/μg of total RNA) in the total RNA was also quantified by SRL Inc. Fukuoka Laboratory using the qRT-PCR method, as described previously (17). Total RNA (1 μg) isolated from the liver samples, as above, was used to quantify hepatic HCV RNA levels using a qRT-PCR assay.

Histopathological examination of liver samples

Histopathological examination of the non-cancerous livers was performed according to the METAVIR scoring system (18). The differentiation of HCC was graded according to the Edmondson and Steiner criteria (grade 1, well differentiated; grade 2, moderately differentiated; and grade 3, poorly differentiated) (19). The pathological stage of HCCs was determined according to the tumour-node-metastasis staging criteria of the International Union Against Cancer and the American Joint Committee on Cancer (20). The histopathological characteristics of the patients are also shown in Table 1.

Statistical analyses

The miR-122 expression is expressed as the median (range) and is presented as box plots. Other continuous variables, including HCV load, are expressed as means ± standard deviation, and presented as scatter plots. Pearson's correlation coefficients were calculated to determine correlations between the serum and hepatic HCV loads. Spearman's rank correlation was used to determine the correlation between miR-122 expression and HCV load, hepatic function (Child–Pugh grades), serum transaminase levels, inflammatory activity, fibrosis stage and serum miR-122 level. The association between miR-122 expression and HCV load was also evaluated for both genotypes (genotypes 1 and 2). Accordingly, it should be considered that the ratio of hepatocytes to other cell types in the specimens could relatively decrease because of the growth of cells other than hepatocytes, such as lymphocytes, macrophages, fibroblasts, stellate cells and myofibroblasts, as liver damage progresses. Thus, it is possible that the expression of liver specific miR-122 may be underestimated in severely damaged liver samples. To eliminate a possible effect of non-hepatocyte cells, a stratified analysis was also performed according to grades of inflammation activity (A0/1, A2, A3) and fibrosis stage (F0/1, F2/3, F4). The Mann–Whitney *U*-test was used to determine differences in miR-122 expression between two groups. The Breslow–Gehan–Wilcoxon test was used to evaluate differences in miR-122 expression between the HCCs and the paired non-cancerous livers. *P*-values < 0.05 were considered to be statistically significant. All statistical analyses were performed using STATVIEW® 5.0 software (Abacus Concepts, Berkeley, CA, USA).

Results

Serum and hepatic hepatitis C virus load

Overall, 185 patients were seropositive for the HCV antibody. Of these, 151 patients were positive for serum HCV RNA and 31 patients were negative for serum HCV RNA (Table 1). In the 151 seropositive patients, the mean serum HCV load was 5.6 ± 0.7 log IU/ml, the mean hepatic HCV load was 6.0 ± 1.0 log copies/μg of total RNA; the hepatic HCV load in two cases was below the measurable limit (2.3 log copies/μg of total RNA). The serum HCV load was positively correlated with the hepatic HCV load ($r = 0.531$, $P < 0.0001$; Fig. 1A). The strength of the correlation was similar to that in a previous report ($r = 0.689$, $P = 0.004$, $n = 15$) (21).

Association between hepatic microRNA-122 expression and hepatitis C virus load

The median hepatic miR-122 expression in all non-cancerous cases was 0.34 (range, 0.02–3.36; $n = 204$), relative to the control sample by qRT-PCR. The median non-cancerous hepatic miR-122 expression in the HCV-infected group and control group was 0.32 (range, 0.02–3.36; $n = 185$) and 0.61 (range, 0.31–2.50; $n = 19$) respectively. We analysed the correlation between the hepatic miR-122 expression and the serum and hepatic HCV loads in non-cancerous samples. The expression of hepatic miR-122 in non-cancerous liver tissue was weakly but positively correlated with the serum HCV load ($\rho = 0.19$, $P < 0.05$; Fig. 1B), but not with the hepatic HCV load ($\rho = -0.14$, $P = 0.08$; Fig. 1C). Furthermore, the expression of hepatic miR-122 in non-cancerous serum HCV-negative patients ($n = 31$) was significantly higher than that in the serum HCV-positive patients ($n = 151$) ($P < 0.0001$) and similar to that in the control cases (Fig. 1D). The association between miR-122 expression and HCV load was analysed for both genotypes 1 and 2. In patients with genotype 1, hepatic miR-122 expression was not correlated with the serum HCV load ($\rho = 0.14$, $P = 0.16$; Fig. 2A) and was weakly and